THE UNIVERSITY OF MICHIGAN

INDUSTRY PROGRAM OF THE COLLEGE OF ENGINEERING

THE EFFECT OF CENTRIFUGAL FORCE ON THE DECONTAMINATION FACTOR IN THE EVAPORATION OF RADIOACTIVE SOLUTIONS

Gerald Hugh Golden

A dissertation submitted in partial fulfillment
of the requirements for the degree of
Doctor of Philosophy in The
University of Michigan
1959

September, 1959

IP-383

Doctoral Committee:

Professor Lloyd E. Brownell, Chairman
Professor Henry J. Gomberg
Professor William Kerr
Professor Joseph J. Martin
Professor W. Wayne Meinke

TABLE OF CONTENTS

TABLE OF CONTENTS (CONT'D)

LIST OF TABLES

LIST OF FIGURES

I. INTRODUCTION

Unique problems arise often in the design of equipment for processing chemical systems that are radioactive. An important example of such a problem is met in connection with the concentration of radioactive aqueous solutions. These solutions are formed in large quantities in the processing of spent nuclear reactor fuel elements and the production of radioisotopes. It is often desirable to concentrate such a solution in order to isolate certain of its constituents or else to reduce its volume prior to storage. In either case, the radioactivity level of the by-product water formed must be below a certain level if the water is to be released to the environment.[5,14] Hence, the production of high-purity by-product water may be a major factor in designing processing equipment for concentrating radioactive aqueous solutions. The amount of carry-over of a given radioisotope from the initial solution to the by-product water is usually measured in terms of the decontamination factor; this is defined as the ratio of the specific activity of the initial solution to the specific activity of the by-product water. Thus, the problem may be alternatively stated as that of designing a concentrating apparatus in which a high decontamination factor is realized.

There are a number of techniques that are used to concentrate radioactive aqueous solutions, such as ion exchange, co-precipitation and evaporation. In the ion exchange technique all cations and anions, including those that are radioactive, are removed from the solution by interaction with cationic, anionic or mixed ion exchange beds. The decontamination achieved by such a system depends upon a number of factors such as the concentration of each component of the feed solution, the

extent of saturation of the bed at a given instant with respect to a given ion, the flow rate of the feed solution through the bed, the bed geometry and the nature of the ion exchange material. Decontamination factors for ion exchange systems usually vary from about 10^2 to 10^4.[7,10,19] In the co-precipitation technique a flocculent precipitate such as aluminum or ferric hydroxide is used to carry down the cations in the solution; this gives about the same decontamination factor range as does the ion exchange method.[1] In the evaporation technique, water is removed from the initial solution by vaporization in a distillation apparatus or an evaporator. The decontamination factor achieved in such equipment varies from about 10^3 to 10^7, depending upon its design and the conditions under which it is operated. Thus, if it is desired to achieve as high a decontamination factor per stage of concentration as is possible, concentration by evaporation is usually employed.

It would be convenient to employ conventional distillation units and evaporators for concentrating radioactive solutions, but it has been found that without modification such units give decontamination factors of only 10^3 to 10^4.[2,5,6,11,13] The reason for this is that the vapor produced carries with it entrained radioactive particulates that contaminate the by-product water. These particulates are either solids such as pieces of rust that have adsorbed activity on their surface or else they are small droplets of the feed solution itself.[5,8] The exact mechanism by which these particulates are formed is not known, but it is intimately associated with the agitation of the liquid surface by bursting bubbles of vapor and the motion of the vapor stream past the liquid surface. By incorporating devices to remove these particulates

from the vapor, it is possible to modify conventional evaporation equipment so that it yields decontamination factors of the order of 10^7.

Several devices have been investigated for removing entrained particulates from the vapor stream. These include cyclone separators and vapor dome baffles placed in the evaporator head, auxiliary bubble-cap and Raschig Ring-packed columns and fiberglass filters. It has been found that for a vapor compression evaporator operating with a cyclone separator in the vapor dome, the decontamination factor varies from 4.1×10^3 to 1.3×10^5.(6) The same evaporator operating with a vapor dome baffle gives decontamination factors varying from 1.0×10^4 to 1.6×10^5.(6) The use of a bubble-cap distillation column in conjunction with a submerged coil evaporator has been shown to give an average decontamination factor of 6×10^6.(5) The same evaporator used with a tower packed with Raschig Rings gives an average decontamination factor of 9×10^5.(5) Decontamination factors of better than 10^7 have been obtained using either of the two evaporators above in conjunction with a fiberglass filter in the vapor line.(5,6) It has been stated that cyclone separators, vapor dome baffles, bubble-cap columns and Raschig Ring-packed columns are effective in removing particulates that are greater than 100 microns in diameter, but that for submicron-particulate removal it is necessary to employ filters such as fiberglass.(8)

The centrifugal evaporator was conceived by Professor L. E. Brownell of the University of Michigan as an apparatus in which droplet entrainment by the vapor may be suppressed by centrifugal force. In essence, the machine consists of a vertical rotating aluminum drum which is externally heated by means of a steam jacket or electrical heaters

in an air jacket. The feed solution is fed into the evaporator through the hollow upper shaft, the vapor is withdrawn through the hollow lower shaft, and the liquid residue is withdrawn through a collecting system at the bottom of the machine. At low rotational speeds, bubble formation will occur in the liquid flowing down the inner wall of the evaporator, ejecting droplets of the liquid into the vapor. Some of these droplets will be carried back into the liquid film by centrifugal force, the carry-back increasing with increasing rotational speed. At a sufficiently great speed, bubble formation will be entirely suppressed due to the establishment of a centrifugal pressure gradient in the liquid, and vaporization will occur only at the free surface of the liquid film.

The prototype centrifugal evaporator was built by the Baker Perkins Company of Saginaw, Michigan, and given to the Michigan Memorial Phoenix Project for evaluation. This machine (see Figure 2) has a stainless steel rotating drum twelve inches in diameter and 23 inches high. It is steam heated and is driven by a 1.5 h.p. motor connected to a variable speed motor pulley. A more detailed description of the prototype evaporator is found in the thesis of J. Ray[22] who made a study of its heat transfer characteristics. Decontamination factors for this unit were measured by S. Aiba[21] using phosphorus-32 as the radioisotope. In this work the specific activity of the condensed vapor was determined by the evaporation method. These data exhibited such a large degree of scatter that it was not possible to determine any consistent effect of the speed of rotation upon the decontamination factor. This scatter may be ascribed to one or a combination of four factors:

1. The use of phosphorus-32 as a phosphate as the radioisotope tracer (see Section IV).
2. The inherent design of the prototype evaporator.
3. Inaccuracies associated with the method used for measuring the specific activity of the condensate.[3]
4. The relatively high vaporization rates studied (see Section IX).

The research program reported in this thesis began with the design of an improved system for measuring the specific activity of the condensate from the evaporator. It was decided to employ a technique developed for the measurement of radioactive contaminants in water[20], in which the solution whose activity is to be determined is passed through an ion exchange bed surrounding a Geiger tube. At a constant feed rate to the ion exchange bed, the rate of increase of count rate in the bed is a measure of the specific activity of the solution (condensate). The design of this counting system is quite critical when it is used to measure the activity of a pure beta-emitting isotope, due to the relatively large linear absorption coefficient for the beta particles in the bed (see Section V). Such a counting system was developed and calibrated (see Section VI) as the initial phase of this research.

Tests were then begun upon the prototype centrifugal evaporator employing the new counting system, but it was soon discovered that serious problems were arising due to leakage of the rotating mechanical seals in this machine. An attempt was made to solve these problems by replacing the seals, but the leakage persisted. It was finally concluded that the most satisfactory solution would be the construction of a modified form of the evaporator in which there were no rotating mechanical

seals. In order to achieve this, it was necessary to eliminate the steam jacket; instead, electrical resistance heaters in an air jacket were employed. Also, it was necessary to modify the system for removing the liquid residue from the evaporator. A stator (see Figure 5) was designed to accomplish this, and then the entire evaporator was fabricated from aluminum in the Instrument Shop of the Phoenix Laboratory at the University of Michigan (see Figure 3).

After putting the modified evaporator into operation, it was discovered that the stator for collecting the liquid residue would often bind with the rotating evaporator body when the unit operated at maximum speed. Also, data indicated such a low decontamination factor that it was felt that the stator probably caused enough agitation of the liquid in the bottom of the evaporator to inject droplets of the active liquid into the vapor. It was decided that the principle of the centrifugal evaporator could not be investigated successfully as long as this possibility existed, and therefore, the liquid residue collecting system was changed to its present modification. This consisted of removing the stator and drilling two No. 41 (0.0960-inch) holes at 45-degree angles on opposite sides through the bottom of the evaporator (see Figure 4). The liquid residue was ejected from the evaporator through these holes and collected in a pan surrounding the entire bottom of the machine. Subsequent testing confirmed the improvement produced by this design of collector.

A preliminary series of inactive and active runs was made in order to locate and correct any potential sources of trouble in the system. From these runs, it was found that the original pump selected,

a centrifugal unit with a cast iron housing, had rusted and contaminated the feed solution. This pump was replaced by a peristaltic pump employing Tygon tubing. It was also found that if carrier-free strontium-89 in distilled water was employed as the feed solution, after several runs about half of the strontium would be adsorbed on the walls of the evaporator and associated flow equipment. To eliminate this problem the feed solution was made 3×10^{-4} molar in strontium nitrate using stable strontium. Finally, the problem of severe corrosion of the inner surface of the evaporator arose. This caused the production of a large amount of an aluminum hydroxide precipitate in the feed solution; the precipitate was found to have more than 90% of the total strontium in the solution occluded onto its surface. The evaporator wall was replaced, and to eliminate further corrosion due to galvanic action, all copper tubing in the feed flow system was replaced by aluminum tubing. After completing these modifications, the entire system was found to be operating satisfactorily and the final test runs of the evaporator were made. This thesis reports the results of those runs, and presents a theory to describe the mechanism of decontamination in the centrifugal evaporator.

II. THEORY OF THE CENTRIFUGAL EVAPORATOR

A liquid may undergo evaporation by a surface type or a nucleate mechanism. In the former, vaporization occurs just at the liquid-vapor interface, as for example evaporation from the surface of a quiet pond at ambient temperature. In the latter, irregularities in the containing surface, as well as small particles in the liquid, form regions of reduced surface tension and, hence, reduced vapor pressure. Bubbles of vapor may be nucleated in these regions if the liquid is near or at its saturation temperature; these bubbles increase in size until they reach the free surface of the liquid. There the bubbles burst and the bubble film contracts as a result of surface tension to produce small droplets of liquid that are thrown into the vapor. If it is desired to produce a vapor that is free of (non-volatile) material found in the liquid, droplet injection into the vapor must be eliminated or drastically reduced. A calculation is made in Appendix A to show the magnitude of this contaminating effect. It is seen that if one drop, having a volume of 0.05 milliliters, is injected into 100 liters of saturated vapor, the decontamination factor (ratio of specific activity of liquid to specific activity of condensed vapor) is reduced from 10^7 to 10^3.

As stated in the Introduction, it has been found possible to remove liquid droplets from the vapor stream coming from conventional evaporators by employing cyclone separators, vapor dome baffles, bubble cap columns, Raschig Ring columns, glass wool columns, or combinations of these.[5,6,8] The centrifugal evaporator has been conceived as an apparatus in which centrifugal force is used to de-entrain liquid droplets from the vapor stream when nucleate evaporation does occur, and in which

the application of sufficient centrifugal force may shift the evaporation mechanism from the nucleate to the surface type. In this section, a derivation is presented for the decontamination factor, assuming evaporation by the nucleate mechanism. A derivation is also presented for the criterion for surface evaporation to occur.

Consider one (spherical) droplet of liquid of diameter D, in the vapor at a distance r from the axis of rotation of the centrifugal evaporator. The force acting in the direction of the evaporator wall from the axis of rotation is considered to be positive. The forces acting upon the droplet in the horizontal direction are:

1. The centrifugal force tending to carry the droplet to the evaporator wall: $F_c = m_\ell \omega^2 r = \frac{\pi D^3}{6} \rho_\ell \omega^2 r$.
   Here m_ℓ is the mass of the droplet, ρ_ℓ is its density, and ω is the angular velocity of the evaporator.
2. The frictional force due to the vapor moving toward the axis of rotation and tending to carry the droplet with it. Here assume the droplet to be in laminar flow, for which case Stokes' Equation applies: $F_R = -3\pi D \mu v$.
   Here μ is the viscosity of the vapor and v is the velocity of the droplet relative to the vapor.

Then:

$$\frac{\pi D^3}{6} \rho_\ell \frac{dv}{dt} = \frac{\pi D^3}{6} \rho_\ell \omega^2 r - 3\pi D \mu v$$

$$\frac{dv}{dt} = \omega^2 r - \frac{18 \mu v}{D^2 \rho_\ell} \quad .$$

If the droplet reaches its terminal velocity, then:

$$\frac{dv}{dt} = 0 = \omega^2 r - \frac{18\mu V}{D^2 \rho_\ell},$$

or:

$$V_T = \frac{\rho_\ell \omega^2 D^2 r}{18\mu}.$$

Consider next the flow of the vapor. Let the total mass flow rate of vapor be $\dot{W}$. The volumetric flow rate toward the axis of rotation is $\dot{W}/\rho_v$, where ρ_v is the vapor density. If the lateral area normal to the vapor flow at $\underline{r}$ is $2\pi rL$, then the vapor velocity is:

$$V_v = \frac{\dot{W}}{2\pi r L \rho_v}.$$

The criterion for the droplet to be entrained is:

$$V_T < V_v,$$

or:

$$\frac{\rho_\ell \omega^2 D^2 r}{18\mu} < \frac{\dot{W}}{2\pi r L \rho_v} \Rightarrow D^2 < \frac{18\mu \dot{W}}{2\pi r^2 \omega^2 L \rho_v \rho_\ell}.$$

This criterion gives the maximum diameter of a droplet at $\underline{r}$ that is flowing toward the axis of rotation of the evaporator, as a function of $\dot{W}$ and ω. Any droplets having diameters greater than that given by this criterion will be de-entrained from the vapor stream.

Let $\dot{V}$ be the total volumetric rate of flow of droplets toward the axis of rotation of the evaporator. Then, since the droplets do not decrease in volume by evaporation as they move in the vapor, the specific activity of the (condensed) vapor, S_g, is evaluated as a function of the

specific activity of the liquid, S_ℓ:

$$S_s = \frac{\dot{V} S_\ell}{\frac{\dot{W}}{\rho_\ell} + \dot{V}} \approx \frac{\dot{V} S_\ell \rho_\ell}{\dot{W}} . \qquad \text{for} \qquad \frac{\dot{W}}{\rho_\ell} \gg \dot{V}$$

The decontamination factor, D.F., is:

$$D.F. \equiv \frac{S}{S_s} = \frac{\dot{W}}{\dot{V} \rho_\ell} .$$

In order to evaluate $\dot{V}$, it is necessary to know the distribution of droplets throughout the volume of the evaporator. Assume that the droplets are injected into the vapor in a given distribution in diameter, and attain their terminal velocities after travelling a very short distance toward the axis of rotation. For purposes of correlation, assume that this distance is zero. Then at r_2 only those droplets are entrained whose diameters are such that:

$$D^2 < \frac{18 \mu \dot{W}}{2\pi r_2^2 \omega^2 L \rho_v \rho_\ell} \qquad (r_2 = \text{inner radius of evaporator}).$$

At a smaller radius droplets of larger diameters could become entrained, except that they have already been removed at the larger radius, r_2. Alternatively stated, the distribution in diameter of the droplets is independent of $\underline{r}$ everywhere but at $r = r_2$, where the initial distribution is established. Let $N(D,r_2)$ be the droplet current or number of droplets per unit area normal to the direction of flow having diameters between D and D + dD that flow toward the axis of rotation in unit time.

Then:

$$\dot{V} = \int_0^{D_m(r_2)} \frac{\pi D^3}{6} N(D, r_2) \cdot 2\pi r_2 L \, dD$$

$$= \frac{\pi^2 r_2 L}{3} \int_0^{D_m(r_2)} D^3 N(D, r_2) \, dD .$$

where:

$$D_m(r_2) = \left[\frac{18\mu \dot{W}}{2\pi r_2^2 \omega^2 L \rho_v \rho_l}\right]^{\frac{1}{2}} = \left[\frac{18\mu \dot{W}}{2\pi L \rho_v \rho_l}\right]^{\frac{1}{2}} \frac{1}{r_2 \omega} .$$

As a first approximation set $N(D,r_2) = N_o$, a constant. Thus:

$$\dot{V} = \frac{\pi^2 r_2 L}{3} \int_0^{D_m(r_2)} D^3 N_o \, dD = \frac{\pi^2 r_2 L N_o}{3} \left[\frac{D^4}{4}\right]_0^{D_m(r_2)}$$

$$= \frac{27\mu^2 \dot{W}^2 N_o}{r_2^3 \omega^4 L \rho_v^2 \rho_l^2} .$$

and

$$D.F. = \frac{\dot{W}}{\dot{V} \rho_l} = \frac{r_2^3 L \rho_v^2 \rho_l \omega^4}{27\mu^2 \dot{W} N_o} .$$

For $\dot{W}$ and r_2 fixed,

$$D.F. = K\omega^4 .$$

This equation predicts that as ω approaches zero, the decontamination factor approaches zero, a situation that is not meaningful physically because the decontamination factor for any evaporative system is always greater than unity. Also, examination of the experimental data shows that the decontamination factor exhibits a less than fourth-power dependence upon the angular velocity of the evaporator for the range of angular velocities studied. The significance of this with respect to the distribution function $N(D,r_2)$ is believed to be that the preponderence of

droplets injected into the vapor have diameters less than D_m, because fewer droplets are de-entrained at a given value of ω than would be if the average diameter were equal to D_m. For this reason, a distribution function must be sought that starts at the origin, peaks rather rapidly and then decreases asymptotically to zero. The most obvious example of such a function is the Poisson distribution. However, the Poisson distribution is not a continuous function and, hence, cannot be integrated. As an alternative, consider the function:

$$X^{-5} e^{-\frac{1}{X}} .$$

Sketches of X^{-5}, $e^{-\frac{1}{X}}$, and $X^{-5}e^{-\frac{1}{X}}$ are shown in the diagram below.

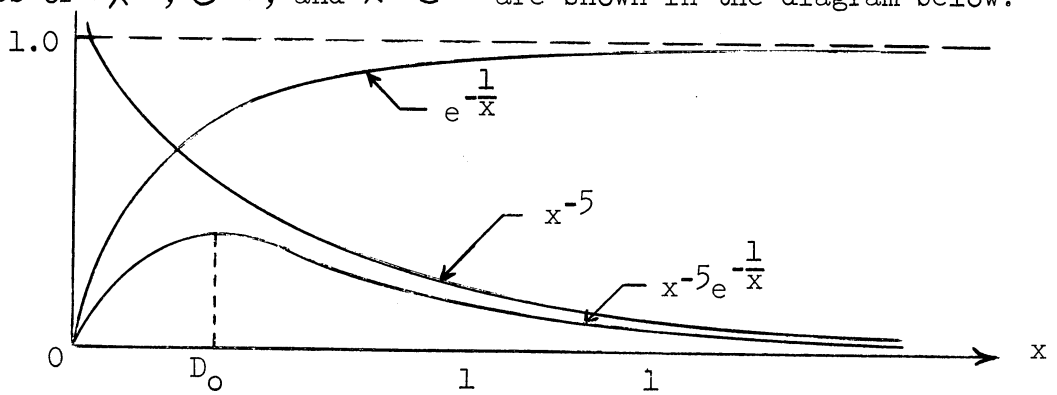

Plots of x^{-5}, $e^{-\frac{1}{x}}$ and $x^{-5}e^{-\frac{1}{x}}$ vs. x

The function $X^{-5}e^{-\frac{1}{X}}$ must be tested for continuity at $X = 0$.

$$\mathcal{L} = \lim_{X \to 0+} \frac{e^{-\frac{1}{X}}}{X^5} \quad ; \quad \text{set} \quad \frac{1}{x} = u$$

$$\mathcal{L} = \lim_{u \to \infty} \frac{e^{-u}}{(\frac{1}{u})^5} = \lim_{u \to \infty} \frac{u^5}{e^u} = 0.$$

Thus, set:

$$N(D, r_2) \equiv N_o D^{-5} e^{-\frac{a}{D}} .$$

Now:

$$\frac{d}{dD}(D^{-5}e^{-\frac{a}{D}}) = ae^{-\frac{a}{D_o}}D_o^{-7} - 5e^{-\frac{a}{D_o}}D_o^{-6} = 0.$$

$$D_o^{-6}\, e^{-\frac{a}{D_o}}\left[aD_o^{-1} - 5\right] = 0.$$

But:

$D_o^{-6} = 0 \Rightarrow D_o \to \infty$, a root of non-interest

$e^{-\frac{a}{D_o}} = 0 \Rightarrow D_o = 0$, another root of non-interest.

Hence:

$$aD_o^{-1} = 5\ ;\quad a = 5D_o\ ;\quad D_o = a/5.$$

Here, D_o is the most probable diameter of a given droplet in the chosen distribution.

Using this distribution function it is now possible to evaluate $\dot{V}$:

$$\dot{V} = \frac{\pi^2 r_2 L}{3}\int_0^{D_m(r_2)} D^3 N(D, r_2)\,dD = \frac{\pi^2 r_2 L}{3}\int_0^{D_m(r_2)} D^3 N_o D^{-5} e^{-\frac{a}{D}}\,dD$$

$$= \frac{\pi^2 r_2 L N_o}{3}\int_0^{D_m(r_2)} D^{-2} e^{-\frac{a}{D}}\,dD.$$

Set:

$$u = \frac{a}{D}\ ;\quad D = \frac{a}{u}\ ;\quad dD = -\frac{a}{u^2}\,du$$

$$\dot{V} = \frac{\pi^2 r_2 L N_o}{3}\int_{\infty}^{a/D_m(r_2)} \frac{u^2}{a^2} e^{-u}\left(-\frac{a}{u^2}\,du\right)$$

$$= \frac{\pi^2 r_2 L N_o}{3a}\int_{a/D_m(r_2)}^{\infty} e^{-u}\,du.$$

$$= \frac{\pi^2 r_2 L N_o}{3a} e^{-a/D_m(r_2)}$$

$$= \frac{\pi^2 r_2 L N_o}{15 D_o} e^{-5 D_o \left(\frac{2\pi L \rho_v \rho_l}{18 \mu \dot{W}}\right)^{\frac{1}{2}} r_2 \omega} .$$

and:

$$D.F. = \frac{\dot{W}}{\dot{V} \rho_l} = \frac{15 D_o \dot{W}}{\pi^2 r_2 L N_o \rho_l} e^{5 D_o \left(\frac{2\pi L \rho_v \rho_l}{18 \mu \dot{W}}\right)^{\frac{1}{2}} r_2 \omega} .$$

Here it is seen that if $\omega = 0$,

$$D.F. = \frac{15 D_o \dot{W}}{\pi^2 r_2 L N_o \rho_l} > 0.$$

The assumptions upon which this derivation is based, merit further discussion. These assumptions are:

1. The droplets are spherically shaped. This assumption is valid for droplets of small diameters moving at low velocities relative to the vapor.
2. The angular velocity of the droplets is the same as that of the evaporator. This is equivalent to the assertion that there is no slippage at the liquid-vapor interface. This assumption is valid at low angular velocities and becomes increasingly erroneous at higher angular velocities.
3. The droplets are in laminar flow. This is equivalent to saying that $|v_V - v_T|$ is small, which appears to be reasonable, considering that the droplets are of small size and

the relative velocities are distributed around the value zero at a given point in the vapor.

4. The droplets reach their terminal velocities a very short distance from the liquid vapor interface where they originate. To compute the actual value of this distance, it would be necessary to know the velocity with which each droplet is ejected into the vapor, an extremely complex problem. But the small mass and diameter of the droplets indicates that their terminal velocities are reached rapidly.

5. A one-dimensional force and vapor flow model is assumed. This is because a three-dimensional treatment would only attempt to refine the theory beyond the precision of the experimental data obtainable.

It is instructive to consider each of the terms that enter into the equation derived for the decontamination factor in order to test that equation in a qualitative manner. Due to the one-dimensional de-entrainment model employed, it might seem strange that the final expression for the decontamination factor should depend upon L, the length of the evaporator. However, the total rate of vapor production in the evaporator, $\dot{W}$, is directly proportional to the lateral area of the evaporator (if the entering feed solution is at its saturation temperature) which is proportional to L. That is, $\dot{W}/L = \dot{W}'$, the rate of production of vapor per unit height of the evaporator, is constant, giving:

$$D.F. = \frac{15 D_o \dot{W}'}{\pi^2 r_2 \rho_\ell N_o} e^{5 D_o \left(\frac{2\pi \rho_v \rho_\ell}{18 \mu \dot{W}'}\right)^{\frac{1}{2}} r_2 \omega}$$

The most probable diameter of a droplet, D_o, is determined by the force acting at the liquid surface when the vapor bubble bursts, and this force is determined largely by the surface tension of the liquid. Since the surface tension depends only upon the liquid surface temperature which is constant because the evaporator operates at essentially atmospheric pressure, it is to be expected that D_o is constant to a first approximation (this point is pursued further in the consideration of the experimental data in Section IX). Thus, since the droplet current, $N(D,r_2)$, increases with increasing $\dot{W}'$ (i.e., v_v), N_o must increase with $\dot{W}'$. If $\dot{W}'$ is increased, the ratio $\dot{W}'/N_o$ does not increase as rapidly as $\exp(1/\dot{W}')^{1/2}$ decreases and, hence, the decontamination factor decreases with increasing $\dot{W}'$, which is borne out by the experimental results of this program. The equation also predicts that if the evaporator radius, r_2, is increased, then at low values of r_2 the decontamination factor decreases, goes through a minimum, and then increases steadily. This may be seen by expanding the equation:

$$D.F. = \frac{C_1}{r_2} e^{C_2 r_2}$$

as a power series about the origin:

$$D.F. = \frac{C_1}{r_2}\left(1 + C_2 r_2 + C_2^2 r_2^2 + \cdots\right) = \frac{C_1}{r_2} + C_1 C_2 + C_1 C_2^2 r_2 + \cdots .$$

The interval $r_2 = 0$ to r_2, corresponding to the minimum decontamination factor, represents an interval in which the simple one-dimensional model of vapor flow breaks down. Beyond the minimum, this equation predicts correctly an increase in the decontamination factor with increasing r_2. This is because as r_2 increases, the vapor velocity decreases and the droplet terminal velocity increases, resulting in a decrease in the amount of entrainment. The breakdown of the one-dimensional vapor flow

model at r_2 small is not of great concern, since for any design of centrifugal evaporator, r_2 would be of a considerable size. The density of the saturated feed solution, ρ_ℓ, is essentially constant, and does not affect the decontamination factor. When considering the effect of the vapor density, ρ_v, upon the decontamination factor, it is necessary to consider the effect of the vapor viscosity, μ, at the same time. This is because the ratio ρ_v/μ appears in the exponential term in the equation. An examination of experimental data for saturated steam shows that in the range 100 - 150°C the density increases at the rate of 1.55%/°C, and the viscosity at the rate of 0.25%/°C. From this it is seen that in this range of temperature, as the saturation temperature (and, hence, saturation pressure) increases for the vapor in the evaporator, the ratio ρ_v/μ increases, and therefore, the decontamination factor increases. This is because the increase in vapor density causes a decrease in the vapor velocity and a corresponding decrease in the entrainment. This suggests an improvement in the decontamination factor by operation at elevated pressures. The increase in vapor viscosity acts to oppose this effect by increasing the drag force acting upon the droplets. Finally, it is seen that the effect of the evaporator angular velocity, ω, upon the decontamination factor is to increase it exponentially.

The equation derived above can be used to predict the decontamination factor only if the parameters D_o and N_o are known as functions of $\dot{W}$ and r_2. It is necessary to determine these relationships experimentally in lieu of an adequate theory describing the mechanism of droplet formation and injection into the vapor. However, this equation

can be used to predict the shape of the curve:

$$D.F. = f(\omega).$$

Set:

$$\frac{15 D_o \dot{W}}{\pi^2 r_2 L \rho_\ell N_o} = \alpha ; \qquad 5 D_o \left(\frac{2\pi L \rho_v \rho_\ell}{18 \mu \dot{W}} \right)^{\frac{1}{2}} r_2 = \beta .$$

Then:

$$D.F. = \alpha e^{\beta \omega}.$$

and

$$\ln(D.F.) = \ln \alpha + \beta \omega.$$

That is, the logarithm of the decontamination factor is predicted to be linear in the angular velocity of the centrifugal evaporator for the distribution function employed.

It is of interest to determine the order of magnitude of the parameters D_o and N_o. This is done by evaluating α and β experimentally for a given $\dot{W}$. For $\dot{W}$ = 10.4 milliliters/minute, a least squares fit (see Section IX) for the thirteen runs made yields:

$$\alpha = 2.47 \times 10^{4}$$

$$\beta = 2.77 \times 10^{-2} \text{ sec.}$$

Also:

$$r_2 = 3.99/12 = 0.333 \text{ ft.}$$

$$L = 15.00/12 = 1.250 \text{ ft.}$$

$$\dot{W} = 10.4 \frac{\text{ml}}{\text{min}} \times \frac{1 \text{ gm}}{\text{ml}} \times \frac{1 \text{ lb}}{454 \text{ gm}} \times \frac{1 \text{ min}}{60 \text{ sec}} = 3.82 \times 10^{-4} \frac{\text{lb}}{\text{sec}} .$$

$$\rho_v = 1/26.80 = 0.0373 \text{ lb}_m/\text{ft}^3.$$

$$\rho_\ell = 1/0.01672 = 59.8 \text{ lb}_m/\text{ft}^3.$$

$$\mu = 125.5 \times 10^{-6} \times 0.0672 = 8.40 \times 10^{-6} \text{ lb}_m/\text{ft sec.}$$

Now:

$$5D_o\left(\frac{2\pi L \rho_v \rho_l}{18\mu \dot{W}}\right)^{\frac{1}{2}} r_2 = \beta = 2.77\times10^{-2} \text{ sec}$$

$$5D_o\left(\frac{6.28\times1.250\times0.0373\times59.8}{18\times8.40\times10^{-6}\times3.82\times10^{-4}}\right)^{\frac{1}{2}}\times0.333 = 2.77\times10^{-2}$$

$$D_o = 0.951\times10^{-6}, \text{ ft}$$

$$\frac{15 D_o \dot{W}}{\pi^2 r_2 L \rho_l N_o} = \alpha = 2.47\times10^{4}$$

$$\frac{15\times0.951\times10^{-6}\times3.82\times10^{-4}}{9.86\times0.333\times1.250\times59.8\,N_o} = 2.47\times10^{4}$$

$$N_o = 8.98\times10^{-16}, \quad \frac{\text{droplets}}{\text{ft}^2 \text{ sec ft}}$$

A. Non-Nucleate Evaporation

In theory, it is possible to eliminate droplet ejection into the vapor by completely suppressing bubble formation in the liquid film undergoing vaporization. This is done by the application of a centrifugal force gradient to the liquid film such that the liquid is at its saturation temperature only at its free surface, and is subcooled throughout its bulk. The following diagram shows a small section of the cylindrical evaporator wall, down which flows the liquid undergoing vaporization. First, assume that the only force acting upon the liquid is that of gravity. If the liquid is in streamline flow, i.e., contains no turbulence, then under steady-state conditions the temperature gradient through it may be approximated by the Fourier equation of heat conduction:

$$q/A = k\,dt/dx.$$

where:

q = rate of heat flow normal to liquid film, Btu/hr.

A = area normal to heat flow (surface area of evaporator), ft^2.

k = thermal conductivity of water, Btu/hr ft^2 °F/ft.

t = temperature in liquid film measured at distance x from free surface of film toward wall, °F.

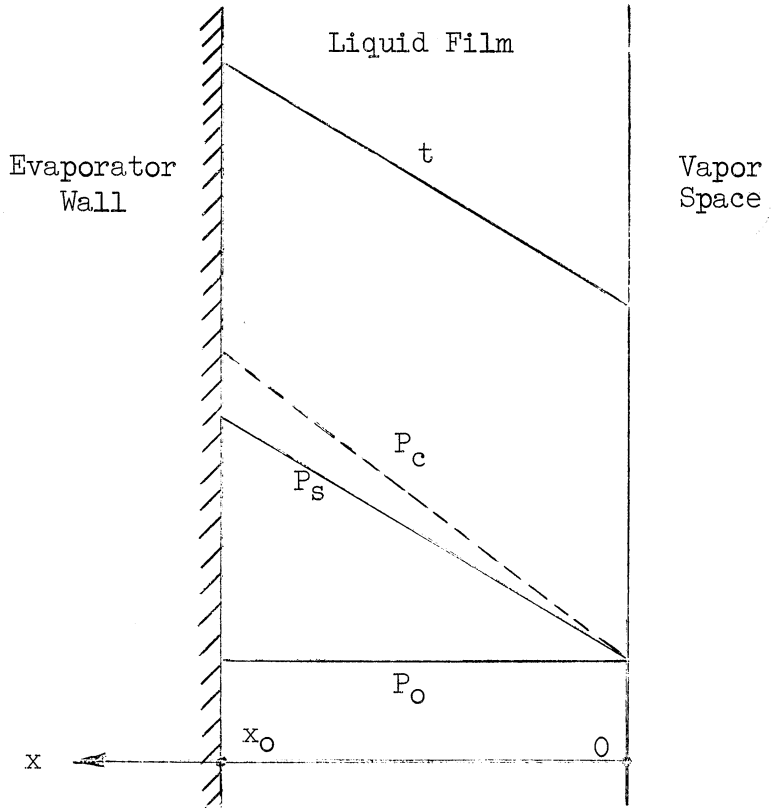

Cross Section of Liquid Film on Evaporator Wall

For x_o, the liquid film thickness, small, $\underline{t}$ is approximately linear in $\underline{x}$ and is shown as the line labelled $\underline{t}$. Corresponding to the temperature at each point in the film is a saturation vapor pressure, which for x_o small is also approximately linear in $\underline{x}$. This is shown as the line labelled P_s. The slope of P_s is governed by the heat flux, but the value of P_s at the free surface (x = 0) is fixed and equal to the

vapor pressure, P_o, of the water in the vapor space (normally, P_o is the total pressure in the vapor space). But the actual pressure in the liquid is everywhere P_o, and thus, for any finite heat flux the liquid bulk is supersaturated. Since the extent of bubble formation increases with the degree of supersaturation of the liquid, and the latter is most supersaturated at the wall ($x = x_o$), nucleate evaporation is likely to occur in this system.

The centrifugal evaporator is designed to establish a centrifugal pressure gradient in the liquid film such that the actual pressure at each point in the liquid is equal to or slightly greater than the vapor pressure due to the heat flow. In Appendix B a derivation is presented for the centrifugal pressure equation:

$$P - P_o \approx \frac{\rho r_2 x}{g_c} \omega^2 \left(\frac{2\pi}{60}\right)^2,$$

where:

P = pressure at point $\underline{x}$ in liquid, lbs_f/ft^2.

r_2 = inside radius of evaporator, ft.

ρ = density of water in liquid film, lbs_m/ft^3.

g_c = conversion factor, 32.2 lbs_m ft/sec^2 lb_f.

This equation shows that the centrifugal pressure gradient varies as the square of the evaporator RPM. From this, it follows that by suitably selecting the RPM the centrifugal pressure line can be made to coincide with the saturation pressure line. By operating at a slightly greater RPM (line P_c) film-type vaporization is assured, and the evaporator will operate optimally. If it is desired to increase the capacity of the machine by increasing the heat flux, the saturation vapor pressure

gradient also increases, and it is necessary to increase the RPM of the machine to maintain surface vaporization.

This result can be derived quantitatively as follows. The heat transfer is given by:

$$\frac{q}{A} = k\frac{dt}{dx} .$$

But:

$$t = aP + b .$$

for a short range of t, and thus:

$$\frac{q}{A} = Ka\frac{dP}{dx} \qquad \text{or,} \quad \frac{q}{AKa} = \left(\frac{dP}{dx}\right)_t .$$

By differentiating the centrifugal pressure equation with respect to x, the following equation is obtained:

$$\left(\frac{dP}{dx}\right)_c = \frac{\rho r_2}{g_c}\omega^2\left(\frac{2\pi}{60}\right)^2 .$$

The criterion for film-type vaporization is:

$$\left(\frac{dP}{dx}\right)_c \geq \left(\frac{dP}{dx}\right)_t .$$

or:

$$q \leq \frac{AKa\rho r_2}{g_c}\omega^2\left(\frac{2\pi}{60}\right)^2 .$$

It should be noted that the above equation is independent of x_o, the liquid film thickness. It follows that according to this derivation the criterion for film-type vaporization is independent of the feed rate to the evaporator, which determines x_o, if the liquid feed entering the machine is at the saturation temperature.

For the actual evaporator studied, the following parameters are fixed:

$$A = 2\pi r_2 l = 2\pi \times 3.99/12 \times 15/12 = 2.61 \text{ ft}^2.$$

$$k = 0.393 \text{ Btu/hr ft } ^\circ\text{F}.$$

$$a = 2.34 \times 10^{-2} \text{ } ^\circ\text{F ft}^2/\text{lb}_f.$$

$$\rho = 59.9 \text{ lb}_m/\text{ft}^3.$$

$$r_2 = 3.99/12 = 0.332 \text{ ft}.$$

$$g_c = 32.2 \text{ lb}_m\text{ft/sec}^2 \text{ lb}_f.$$

Upon substituting these values into the above equation, it reduces to:

$$q \leq 1.622 \times 10^{-4} \omega^2.$$

If the centrifugal evaporator is made to rotate at 1,000 RPM, then:

$$q \leq 1.622 \times 10^{-4}(10^3)^2 = 162.2 \text{ Btu hr}.$$

This corresponds to:

$$162.2 \frac{\text{Btu}}{\text{hr}} \times \frac{1 \text{ lb vaporized}}{970 \text{ Btu}} = 0.1673 \frac{\text{lb vaporized}}{\text{hr}}$$

$$= 1.26 \frac{\text{ml vaporized}}{\text{min}}$$

The maximum allowable vaporization rate computed according to the above criterion will be less than the actual value because of the assumption that the saturation pressure gradient could be derived from the Fourier equation of heat flow. Actually, the Fourier equation as written holds only for a static medium, and any turbulence in the liquid film would have the effect of increasing the thermal conductivity of the water. Such turbulence exists in the liquid film flowing down the inner wall of the evaporator, and hence, the use of the thermal conductivity of

static water in computing the maximum allowable vaporization rate will yield a value lower than the true value. The value of this criterion for surface evaporation is that it predicts the lower limit of the rate of condensation for a given RPM. The actual condensation rate may be considerably higher, and would have to be determined experimentally. Note that the previous calculations predict that the maximum rate of vaporization for non-nucleate vaporization is only about one-tenth of the vaporization rates used experimentally. To obtain non-nucleate evaporation using an experimental ratio of 12.6 ml/min would require an increase in the speed of $\sqrt{10}$, or a speed of about 3300 RPm, which was excessive for the apparatus available.

III. DESCRIPTION OF THE APPARATUS

A sketch of the final modification of the centrifugal evaporator is shown in Figure 4. The body of the evaporator is fabricated from a 15-1/8-inch length of standard eight-inch aluminum pipe that had been squared at each end. The upper head, which is fabricated from one-inch aluminum, has built into it a distributor plate that serves the dual function of carrying the feed solution to the wall and maintaining a liquid seal so tha vapor produced cannot escape through the hollow upper shaft. The lower head (see Figure 6) has two liquid residue egress holes drilled through it and contains the hollow shaft through which the vapor leaves the evaporator. The heads are both grooved to accommodate the body, and are held in place by six 1/4-inch brass tie rods (see Figure 8). Permatex Gasket Cement No. 2 is used as a seal between the heads and the body of the machine. The evaporator rotates in an upper and a lower ball bearing, both of which are completely sealed. The frame surrounding the machine is constructed of aluminum, and this entire assembly rests upon another frame made of angle iron. The pan for collecting the liquid residue ejected from the bottom head of the machine is fabricated from 24-gauge sheet brass that is soft-soldered rather than silver-soldered, to prevent heat distortion of the rolled parts. The entire inside surface of the pan is painted with stovepipe enamel to prevent galvanic interaction between the brass and the outside of the bottom aluminum head. A half-inch drain line in the bottom of the pan collects the liquid residue for return to the feed bottle.

The condenser housing (see Figure 7) is made from a five-inch length of four-inch brass tube, flanged at the open end. A rubber

gasket is used to seal the condenser housing to the bottom of the evaporator housing base plate. The vapor is condensed on the surface of 23 feet of 1/4-inch copper tubing wound into three concentric helices. A half-inch copper tube protrudes up 7/8 inch from the bottom, inside the condenser housing; this serves as a wier to smooth out the flow of the condensate from the condenser to the monitor rotameter. The holdup volume produced by the wier (here, 163.1 milliliters) has a damping effect upon the composition of the condensate leaving the condenser; this effect must be taken into consideration in the operation of the evaporator during the test runs. It is treated in greater detail in Appendix D. A line connected to the cooling water supply is valved into the bottom of the condenser housing to flush out the housing at the beginning of each run. A vent tap is located halfway up the side of the housing; this serves to indicate the presence of too high a water level in the housing during a flushing operation, and also to accommodate pressure variations in the evaporator during startup.

The simplest method for varying the speed of the evaporator is to drive it with a conductively compensated a.c. series motor, powered through an autotransformer. Since this type of motor is used extensively in home vacuum cleaners, one was removed from a Hoover cleaner and tested with the evaporator. It was found to operate entirely satisfactorily when cooled externally by compressed air. A Vee-belt pulley was machined to fit the shaft of the motor which was installed in a bracket connected to the evaporator housing top plate. Another Vee-belt pulley was machined to fit the upper shaft of the evaporator, and the machine was driven by this arrangement. The speed of rotation was measured

by means of a Strobotac (General Radio Corp. Type 631-B). This instrument is capable of measuring RPM's to an accuracy of 1% or better.

The evaporator is heated by a combination of six resistance wire cone heaters, each of which is rated at 660 watts at 110 volts. Each cone is mounted in a six-inch tinned sheet steel funnel to serve as a reflector, and the funnels are mounted symmetrically in the air jacket.

The jacketed Geiger tube used in the counting system was fabricated by the N. Wood Counter Laboratory. It is a thin-walled unit (30 mg/cm^2) twenty millimeters in diameter, and has a deposited silver cathode twenty centimeters long. The tube was filled with a conventional organically quenched counting gas, which gave a threshold voltage of 870 volts and a plateau about 130 volts long. The plateau slope was found to be 5%/100 volts. The jacket was made of 35 millimeter standard pyrex tubing, at the lower end of which the Geiger tube was connected and which necked down at the top to 5/8-inch. A length of six-millimeter pyrex tubing was manifolded into the jacket near the bottom. The entire assembly is mounted on a wooden frame as is shown in Figure 1. This figure also shows an eight-millimeter diameter section of pyrex tubing that is fastened next to the counter. The purpose of this tube is to hold a standard cobalt-60 source that is used to calibrate the counter each time it is used. The activity of this source was adjusted initially to give about 9,000 counts per minute in position in the eight-millimeter tube. The entire counter assembly as shown in Figure 1 is installed in a cylindrical shield having a two-inch thick lead wall, to minimize the background count.

A Nuclear-Chicago Model 186 Scaler is used as the high voltage supply, and for counting the output pulses from the Geiger tube. The output pulses from the scaler are fed into a Radiation Counter Laboratory Linear Count Rate Meter (Mark 15 Model 15), and the count rate output pulse is fed from the count rate meter into a Varian Recorder (Model G-11). The scaler contains a 3,600 cycle pulse calibration supply, and the ratemeter contains a 7,200 cycle supply, both of which are employed in calibrating the recorder.

The feed and monitor rotameters are both Fischer and Porter instruments. The former has a range of 0 to 0.81 gpm, and the latter has a range of 0 to 200 ml/min. The monitor rotameter was calibrated with water, and the calibration curve was found to agree exactly with the curve supplied by the manufacturer. A peristaltic pump is used to circulate the feed solution from the feed to the surge bottle. The use of the latter serves to smooth out the pulsations in the flow that are due to the principle upon which the peristaltic pump operates. Tygon tubing, 7/16-inch O.D. by 5/16-inch I.D. was used in the pump. The tubing was found to withstand the pump action and hot feed solution for at least four runs (about 16 hours of operation) but was replaced at the end of every fourth run.

The wash bottle was employed originally to hold the feed solutions used in calibrating the counting system. After this was completed, the wash bottle was used to hold the hydrochloric acid for eluting the ion exchange column after each run, and then the water for washing the acid out of the column. Also, since about 800 milliliters of water was vaporized from the feed solution (in the collecting pan) during the

course of each run, makeup water was added to the feed bottle through the wash bottle. The inside surface of the wash bottle, counting system, and associated tubing, was coated with a water-repellant organosilicon compound (Siliclad) to prevent deposition of strontium-89 ions on those surfaces.

Valve A is a three-way stopcock; valves B, C, D, E, F, G, H, J, K and L are all Bunsen clamps acting against either rubber or Tygon tubing. It was felt that the use of such clamps provided simple, leak-proof and durable valves. The drain line terminating in valve F was used when flushing the condenser housing with cooling water prior to a run, and also when eluting the ion exchange column with acid as well as when washing it with water. The drain line terminating in valve E was used when 250 milliliters of condensate water was passed from the condenser housing through the counting system just at the start of a run (to ascertain the freedom of the condenser housing from strontium-89). Valve H was used just at the end of a run to withdraw a sample of the feed solution for counting. Valve L was used to vent the surge bottle at the end of a run. During a run, this valve was always closed. The use of the entire system in making a run is described in detail in Section VIII.

This system is designed to operate completely on closed loops; that is, there is no water or strontium-89 taken from or added to the system during a run. Actually, however, some vaporization of the feed does occur in the collecting pan, and it is necessary to add makeup water at the start of a new run. Also, some strontium-89 is lost to the counting system during each run, but this is less than one part in 10^7 of the total activity in the feed solution, and hence, is negligible.

IV. CHOICE OF RADIOISOTOPE

A number of factors had to be considered in selecting the particular radioisotope to be used in evaluating the centrifugal evaporator. In the initial decontamination studies of this machine made by Aiba[21], phosphorus-32 was selected as the radioisotope. This was done for several reasons which are summarized below:

1. Phosphorus-32 is readily available and inexpensive.
2. It emits beta particles having a spectrum of energies, the maximum value of which is 1.71 Mev; this, plus the fact that it is a pure beta-emitter, makes detection and specific activity measurements convenient.
3. A considerable amount of experimental work on evaporation of radioactive solutions has been done using this isotope, thus, it would seem, providing a convenient basis for comparison of results.

However, the chemical form of the phosphorus-32 as received is the orthophosphate. Due to the complexity of the chemistry of aqueous phosphate solutions at elevated temperatures, the rigorous interpretation of decontamination data obtained from such solutions is involved. Also, the fact that most radioisotopes are processed chemically as cations and phosphorus-32 as an anion, weighed against its choice for this study.

Accordingly, a radioisotope was sought that normally exists as a cation in solution, has a relatively short half-life, emits an energetic beta particle, and is preferably a pure beta-emitter. It must also be readily available. A study of the Isotopes Catalog and

Price List, Oak Ridge National Laboratory[15], revealed that strontium-89 meets the above requirements. It has a half-life of 54 days, maximum beta energy of 1.48 Mev, and is a pure beta-emitter. It is received as $SrCl_2$ in hydrochloric acid, and is available at weekly intervals. Finally, decontamination of equipment that has been in contact with strontium-89 is not difficult. For these reasons, this isotope was chosen for the decontamination study of the centrifugal evaporator.

V. DESIGN OF THE COUNTING SYSTEM

The major problem connected with the evaluation of the centrifugal evaporator lay in the development of a suitable technique for determining the specific activity of the condensate coming from the machine. This technique would have to possess the ability to determine solution specific activities as small as 10^{-13} curie/ml. The direct method of making such a determination is to evaporate an aliquot of the solution to dryness on a planchet, and then measure the activity in a counter of calibrated geometry. If the specific activity of the solution is high compared to the counter background, this method poses no problem. If, however, the specific activity of the solution is very small (10^{-13} curie/ml) the determination becomes considerably more complex. A large enough volume of solution to give reasonable counting statistics might be evaporated down and then counted.(3) However, with very low specific activities the evaporation losses during concentration may become significant, and in any case the method becomes quite time consuming. Finally, this method does not provide a continuous check of the performance of the evaporator during the entire course of a run.

An alternative method of concentrating the activity is to pass an aliquot of the solution through an ion exchange bed which absorbs the active anions and cations. A suitable counting system is used to measure the activity of the bed as a function of time or volume of solution passed. By calibrating the apparatus with a solution of known specific activity, the counting efficiency (ratio of observed count rate to known disintegration rate in the ion exchange bed) can be determined. The

same radioisotope would generally be employed for calibrating the apparatus as would be found in the solution whose activity is to be measured, thereby eliminating the effect of the emitted particle nature and energy on the counting efficiency. This method can be applied over a wide range of solution specific activities, since the total activity absorbed by the ion exchange bed is directly proportional to the total volume of solution passed (for constant solution specific activity) which is readily controlled. The advantages offered by the ion exchange technique led to its choice as the method for measuring small solution specific activities in this work.

Since the counting efficiency is a major factor in the design of an ion exchange counting system, the parameters that affect it should be considered before discussing the selection of ion exchange resin, resin bed geometry and detector. In general, the efficiency depends upon the following parameters:

1. The nature and energy of the radiation being counted.
2. The geometry and dimensions of the counting system.
3. The nature and particle size of the ion exchange resin bed.

The effect of the nature and energy of the radiation upon the counting efficiency may be seen by comparing counting of a beta-emitter with counting of a gamma-emitter. The probability that either a beta particle or a gamma photon will be counted is equal to the probability, p_1, that the radiation reaches the sensitive volume of the detector times the probability, p_2, that the radiation interacts with the material of the sensitive volume (which may include the wall of the detector) to produce a count. For a gamma photon starting out in the

direction of the detector, p_1 decreases exponentially with distance in the resin bed. However, the linear absorption coefficient for the photon in the bed is so small that for a system of nominal size, p_1 is close to unity. For a beta particle, p_1 decreases approximately exponentially with distance in the resin bed, but here the linear absorption coefficient is relatively large. Hence, p_1 is considerably less than unity for the beta particle. Once a beta particle does reach the sensitive volume of the detector, it is nearly certain to produce a count, i.e., p_2 is close to unity. For a gamma photon, p_2 is very much smaller. Thus, if the radiation source in the resin bed is very close to the counter, beta counting will be more efficient; but if the source in the bed is a relatively great distance from the counter, gamma counting will be more efficient. The linear absorption coefficient for a beta particle decreases markedly with increasing particle energy, and hence, p_1 increases. That is, the greater the beta energy, the greater is the probability that it will reach the detector, and the greater is the counting efficiency.

Since beta particles are to be counted in this work, the distance from the radiation source to the detector should be kept small to achieve a reasonable counting efficiency. This is the biggest single factor in establishing the geometry and dimensions of the counting system.

The nature and particle size of the ion exchange resin affects the counting efficiency because of the effect of the resin density upon the mean linear absorption coefficient of the actual water-resin mixture. For this reason, a resin whose density is considerably greater than that of water is to be avoided (most ion exchange resins are just slightly more dense than water).

The actual choice of the ion exchange resin is dictated primarily by its ability to absorb the radioisotope quantitatively (better than 99%) and rapidly. If the isotope exists in aqueous solution as a cation, a strong cationic resin is used; if it exists as an anion, a strong anionic resin is used. Chemically, most strong cationic resins are basically copolymers of styrene with varying amounts of divinylbenzene. Treatment of the copolymer with sulfuric acid introduces sulfonic groups into the molecule. Subsequent washing with sodium carbonate produces the sodium form of the resin which is regenerated to the hydrogen form with acid. Many anionic resins are made from the same copolymer by treatment with methyl chloromethyl ether followed by amination. The use of tertiary amines results in strongly basic ammonium resins. The commercial resins of both types consist of small spheres from 20 - 50 mesh in diameter. As supplied, the resins contain about 40% moisture, and have a specific gravity of 0.6 - 0.8. Examples of strong cationic resins are Amberlite IR-120 and Dowex-50. Examples of strong anionic resins are Amberlite IRA-400 and Dowex-1. The properties of these and other suitable resins are found in the literature.(16-18)

The stability of the resin to strong regenerants is also of prime importance. At the end of a run, the resin bed contains all the activity carried over by the condensate during the run. In order to get the background activity of the bed as low as possible for the following run, it is essential to remove almost all of the activity. If a strong cationic resin is used, a 3 - 10% acid solution is usually recommended for regeneration, although more concentrated acid may be

required. The resin should undergo no appreciable attrition loss over several hundred regeneration cycles using such strong acid solutions.

The ion exchange resin selected for the counting system is Analytical Grade Amberlite IR-120 (hydrogen form), supplied by the Rohm and Haas Company (Lot No. 772358). It has been found to remove strontium-89 ions quantitatively and rapidly from aqueous solutions. Also, in preliminary studies it has been found to undergo no observable attrition over about 50 exchange - regeneration cycles using up to 60% sulfuric acid.

The geometry into which the resin bed is packed depends upon a number of factors. First and foremost, it should permit efficient counting in conjunction with the chosen detector. Second, it should permit the use of a conventional design of detector. Third, it should be such that the resin bed is stable under a wide range of flow conditions; that is, a minimum amount of channelling and bed displacement should occur. Non-adherence to this factor may well give rise to nonreproducibility of counting efficiency calibrations. Fourth, the geometry should readily permit regeneration and backwashing of the bed between runs.

Two geometries have been considered. In the first, the detector has a tubular shape, and is surrounded by the ion exchange bed which forms a cylindrical annulus (see Appendix C). This configuration was actually the first to be employed in connection with the ion exchange counting technique.[20] In the second geometry, the resin bed is disc-shaped and has detectors located on both faces to form a sandwich (see Appendix C). The feed to the bed is introduced radially along the

transverse axis of the disc, and the eluent is removed around the rim via a manifold.

The cylindrical annular geometry would be chosen more for its convenience of assembly and operation than for its counting efficiency. Even if the resin bed did not absorb any of the radiation being emitted, the maximum counting efficiency is somewhat less than 50%. This unit cannot be used at all to measure the specific activity of alpha-emitting isotopes, due to absorption of the alpha particles by the resin bed and counter wall. It can be used readily for measuring strong beta-emitters such as phosphorus-32 and strontium-89, but not weak beta-emitters such as tritium and carbon-14. It is not difficult to purchase conventional counters for this type of geometry, or even to modify conventional counters to meet a specific design problem. In designing a resin bed for this geometry, a compromise must be made between two conflicting factors. First, a thin annulus of resin is preferable for all beta counting since the amount of beta-radiation reaching the detector decreases approximately exponentially with the bed thickness. Second, the thinner the annulus, the greater will be the effect of flow irregularities and air bubbles upon the counting efficiency, for a given flow rate of feed solution. Thus, it is necessary to select an annulus of minimal thickness that will give resin bed stability.

The sandwich geometry is visualized as an ultimate design for ion exchange bed counting. If no absorption of the emitted radiation occurred in the resin bed or counter face, the counting efficiency would be essentially 100%. Further, the effect of attenuation of radiation by the resin bed is much less than the corresponding effect in the

cylindrical annular bed. This is because for a given thickness of resin bed, the radiation has to go only about half as far to reach a detector as it would with the cylindrical annular geometry. The sandwich geometry does have the disadvantage that the equipment would all have to be specially designed and constructed, and considerable effort may be required to achieve stable bed performance.

It is not possible to compute exactly the counting efficiency for any desired geometry for several reasons. First, the exact attenuation of the radiation being measured (especially if beta radiation is being considered) by the resin bed cannot be expressed analytically. As an approximation for beta radiation, exponential attenuation is assumed. Second, the measured activity is increased by secondary scattering of beta particles into the detector, as well as by bremsstrahlung produced by energetic beta particles. These effects also cannot be described exactly analytically. Third, the assumption of true three-dimensional isotropic emission of radiation from each element of volume of the resin bed gives rise to nonelementary integrals. Thus, to compute the counting efficiency for a given geometry, it is necessary to make certain simplifying assumptions which affect the accuracy of the result. However, the derived expression should give an accuracy of approximately 25% or better. But just as important, it should show which of the independent variables (design parameters) most strongly affect the magnitude of the efficiency, which is of great importance in designing a specific counting system.

In Appendix C, a derivation is presented for the counting efficiency of the cylindrical annular geometry, assuming beta particles

to be the radiation being measured. The assumptions inherent in the derivation are stated as they are required. The final expression for the counting efficiency is found to be a nonelementary integral which may be evaluated numerically, graphically, etc. A particular example is studied, assuming a detector radius of 1.00 cm, and a resin bed thickness of 0.75 cm. The radiation is assumed to emanate from strontium-89 (T = 54d, E = 1.48 Mev), the mass absorption coefficient for which was determined experimentally. The computation yields a counting efficiency of 1.87% for this geometry. It also shows that all radiation originating at a distance greater than about 0.25 cm from the detector wall contributes less than 5% to the total efficiency.

In Appendix C, a derivation is presented for the counting efficiency of the sandwich geometry. Also, an example is given assuming the same resin bed thickness and radioisotope as in the preceding paragraph. In making this calculation, it is necessary to know the distribution of activity in the resin bed. As an approximation, it is assumed that the activity per unit volume at a point in the bed varies linearly with the distance from the axis along which it is introduced into the bed, being a maximum at the axis and zero at the outer edge of the bed. The activity distribution in the bed is computed from this condition. In order to compute the counting efficiency, it is necessary to assume that if no scattering by the bed occurs, every beta particle emitted will reach one of the two detectors. This assumption is good for points near the central axis, but fails near the outer edge of the resin bed. However, since most of the activity is absorbed near the central axis, the assumption should not introduce a great error into the computation. An

exact derivation of the geometry view factor would lead to a nonelementary integral whose solution would require approximating techniques. Finally, it is necessary to make a simplifying assumption regarding the isotropic emission of the beta particles. It is assumed that the average distance from a point of particle emission in the resin bed to the nearest detector is directly proportional to the minimum distance, and that the proportionality constant, k, is a true constant. Using these assumptions, the counting efficiency is evaluated, and found to depend only upon k, the mean resin bed absorption coefficient, μ, and the thickness of the bed, h. It should be noted that the counting efficiency is independent of the resin bed radius only because of the assumed activity distribution in the bed and constant k.

As an example, the conditions of the cylindrical annular geometry are assumed for the sandwich geometry, and the counting efficiency is computed. It is found to be 13.4%, in comparison with 1.87% for the former. Thus, the sandwich geometry is to be preferred where high counting efficiencies are of paramount importance. The ultimate counting system of this nature would conceivably be a disc-shaped resin bed surrounded by a scintillation detecting system.

The most important single parameter in designing this general type of counting system is, as stated earlier, the thickness of the resin bed. Examination of the equation for the counting efficiency of the sandwich geometry shows that for:

$$\lambda = \mu K h \gg 1 \qquad \text{(See Appendix C)},$$

the counting efficiency varies inversely as the thickness of the resin bed. However, the equation for the counting efficiency of the cylindrical

annular geometry shows an inverse square variation with resin bed thickness. This implies that overestimating the thickness of the bed in the latter case is far more costly in terms of efficiency than in the former case; a factor of prime importance in designing an apparatus.

A preliminary investigation indicated that the problems associated with the design and construction of the sandwich apparatus made its immediate consideration unjustifiable. For this reason, the more conventional cylindrical annular geometry was selected for use in the counting system. The dimensions chosen for this geometry were just those used in the sample calculation (see Appendix C). The actual counting efficiency of this system was later found experimentally to be 2.30%. The calibration procedure is described in another section. The actual counting system is shown in Figure 1.

It is of interest to consider the range of detectability that the ion exchange system chosen permits. There is no theoretical upper limit to the specific activity of a solution that can be measured by this system if an indirect procedure is employed. As more and more activity is deposited on the resin bed, the count rate increases. Each detection system has a practical upper limit at which it may be used; for a Geiger tube, this may be about 30,000 counts per minute. For a $4\text{-}\pi$ counter in the proportional region and a typical scintillation system the upper limit may be around 300,000 counts per minute, depending on the system design and ability to correct for coincident counts. Employing these (or more suitable) maximum count rate figures and the estimated (or calibrated) counting efficiency, the total maximum activity to be tolerated in the resin bed is computed. If it is felt that the solution

volume required to deposit the maximum activity is too small, the indirect procedure mentioned earlier is employed. This consists of diluting the solution with a known amount of pure water and then passing the dilute solution through the bed. Thus, there is no upper limit of detectability to be associated with the ion exchange counting system.

The lower limit of detectability is treated as follows. Let a be the activity per unit volume of the feed solution, V be the volume of feed solution passed through the resin bed, and η be the counting efficiency of the bed. The count rate recorded by the detector (excluding background) is:

$$r_a = aV\eta .$$

If the total count rate (including background) is c, and the background count rate is b, then the standard deviation of the true count rate, σ_a, is given by:

$$\sigma_a^2 = t_a^2 \left(\frac{c}{t_c} + \frac{b}{t_b} \right) \quad ; \quad \text{let} \quad t_a = 1 .$$

Therefore:

$$\sigma_a^2 = \frac{c}{t_c} + \frac{b}{t_b} = \frac{aV\eta}{t_c} + b\left(\frac{1}{t_c} + \frac{1}{t_b} \right) .$$

This equation shows the variation of the standard deviation of the true count rate. For σ_a fixed, it is seen that if a decreases V must increase. Also, by increasing η, either a or V may be decreased without increasing σ_a.

The lower limit of sensitivity is determined by $r_a = aV\eta$. If this is taken to be ten counts per minute, and the maximum volume of solution that is desired to pass through the resin bed is V = 50,000 ml,

then:

$$10 = 50{,}000a\eta, \text{ or}$$

$$a = 2 \times 10^{-4}/\eta \text{ cpm/ml}$$

If η is taken as 0.02, then:

$$a = 1 \times 10^{-2} \frac{\text{counts}}{\text{min ml}} \times \frac{1 \text{ min}}{60 \text{ sec}} \times \frac{1 \text{ curie sec.}}{3.7 \times 10^{10} \text{ counts}}$$

$$= 4.5 \times 10^{-15} \text{ curie/ml.}$$

This result may be varied by selecting different values for V and η.

VI. CALIBRATION OF THE COUNTING SYSTEM

The efficiency of the counting system must be known for a given radiation if the system is to be used to measure the absolute specific activity of a dilute solution of the radioisotope emitting that radiation. The counting efficiency is defined as the ratio of the measured count rate to the actual disintegration rate in the resin bed at a given instant. It is possible to derive an expression for the counting efficiency (see Appendix C), although the result is of limited accuracy. For this reason it is necessary to determine the efficiency experimentally by calibrating the counting system with aliquots of a solution of the radioisotope having a known specific activity. There are a number of potential sources of error in making this calibration, and it is important to know what they are and how to correct for them. They include:

1. Spurious counting by the detector (Geiger tube).
2. Formation of air pockets in the resin bed.
3. Channelling in the resin bed.
4. Formation of radiocolloids in the calibrating solution.
5. Absorption of a fraction of the radioactive cation by the walls of pipettes, volumetric flasks, storage bottles, and the counting system itself.

Spurious counting by the detector is indicated by a combination of three techniques. First, a periodic determination of the counter plateau is made. A shortening of the plateau and increase in its slope indicates that the detector is approaching the end of its useful life. Second, before each run, the detector is used to count the activity of

a secondary standard source. An abnormal deviation from the known true count rate is an indication of malfunctioning by the scaler or detector. In this work, a cobalt-60 source giving about 9,000 counts per minute in the counting position, is used as the standard. Third, the counting rate of the detector is recorded continuously during each run. This record is examined periodically for unusual pips in the curve, which would indicate spurious counts.

The formation of air bubbles in the ion exchange resin bed may seriously affect the measured count rate, because the air reduces the mean linear absorption coefficient of the bed. Since the coefficient for air (0.00989 cm^{-1}) is much smaller than the coefficient for the water and resin mixture (7.65 cm^{-1}), a small volume of air in the bed may increase appreciably the measured count rate, and hence, the measured counting efficiency. To prevent bubble formation in the bed, it is necessary that any solution passed through the counting system be deaerated. This includes the calibrating solution, the regenerant, and the wash water.

Channelling in the resin bed is the formation of localized regions of abnormally great solution flow rate. It appears to be a transient phenomenon dependent upon the bed geometry, shape and size of the resin particles and fluid flow rate. It is believed that channelling is the main reason for the variation from one calibration run to the next of the measured counting efficiency. An attempt has been made in all runs to minimize this effect by maintaining the calibration solution feed rate at a reasonably low level (less than 30 ml/min).

Experimental work has shown that if the radioactive ion in solution forms a radiocolloid, it is not taken up quantitatively by the exchange resin.[10] The most convenient way to prevent colloid formation is to use only deionized water in making up the various solutions that are passed through the counting system. All water employed in the calibration runs was deionized in a Laboratory Model Barnstead Demineralizer which produced a product having a conductance equivalent to less than 0.1 ppm of sodium chloride.

It is known that the walls of an untreated glass vessel tend to absorb radioactive cations from a carrier-free solution contained in the vessel. This effect can be eliminated by coating the vessel walls with a water-repellant organosilicon compound (e.g., Desicoat, Siliclad). All volumetric glassware, storage flasks and the detector vessel were treated with Siliclad and then thoroughly rinsed and dried prior to use.

The strontium-89 calibration solutions were prepared by diluting a standard solution whose specific activity was determined previously by 4-π counting (see Section VII). In preparing and manipulating these solutions, all the precautions just outlined were adhered to rigorously. Twelve calibration runs were made, and from each of these the counting efficiency was computed. The arithmetic mean of these twelve values was taken as the efficiency of the counting system. A least-squares fit of the data was also made and yielded an efficiency that differed from the arithmetic mean by less than 0.5%.

The preparation of the calibration solutions was carried out as follows. The first strontium-89 solution as received from Oak Ridge

National Laboratory was diluted to a total volume of 5,000 milliliters (solution A). Nine milliliters of this solution were withdrawn and reserved for the 4-π counting described elsewhere (see Section VII). One more milliliter of solution was withdrawn and diluted to a total volume of 1,000 milliliters (solution B); it was from this solution that all the calibration solutions were prepared. In all the activity measurements made on the strontium-89, it was necessary to correct for radioactive decay due to the relatively short half-life of the isotope (54 days). As a convenience, all activities reported were corrected back to the datum of May 15, unless otherwise indicated. The specific activity of Solution A was 1.16×10^{-6} curie/ml, and that of Solution B was 1.16×10^{-9} curie/ml. In preparing the feed solution for each of the first six calibration runs, 40 milliliters of Solution B was diluted to 4,000 milliliters, giving a specific activity of 1.16×10^{-11} curie/ml or 25.7 counts/min ml. (This corresponded to a decontamination factor of 10^5.) The seventh, eighth and ninth runs were made with solutions whose specific activity was 3/4 of that used in the first six runs. The tenth and eleventh runs were made with solutions one-half as active, and the last run with a solution one-fourth as active as that of the first six runs.

The procedure for making a calibration run is as follows:

1. The resin bed is prepared by first backwashing it with a 10% hydrochloric acid solution to remove the strontium-89, deposited during the previous run.
2. 3,500 milliliters of deaerated and deionized water is backwashed through the bed to flush it of residual acid.

3. 500 milliliters of deionized and deaerated water is passed slowly through the resin bed in the forward direction to prepare it for the run.
4. 150 milliliters of feed solution is passed through the system to remove the "dead" volume of inactive water.
5. The initial activity of the bed is determined. This is somewhat greater than the background activity because the resin bed absorbs a small amount of activity from the 150 milliliters of active solution just passed into it.
6. The detector is calibrated against the standard cobalt-60 source, after which the run is begun.
7. At the end of the run (in all cases 3,850 milliliters of active solution are passed through the system during the run), the final count rate is determined and the recorder is calibrated.

The counting efficiency for a given calibration run is computed from the equation:

$$\eta = \frac{100(r_f - r_i)}{V e^{-0.01283t} S} ,$$

where:

η = counting efficiency, %.

r_f = measured bed activity at end of run, cpm.

r_i = measured bed activity at start of run, cpm.

V = volume of feed solution passed (3,850 ml).

t = elapsed time from May 15, 1958, to time of run, days.

S = known specific activity of feed solution (referred to May 15, 1958) cpm/ml.

The results of the twelve calibration runs are summarized in Table I.

TABLE I

RESULTS OF COUNTING EFFICIENCY CALIBRATIONS

Run No.	Net Co-60 Count, cpm	Bkgrnd. for Run, cpm	Volume Passed	Final Count Rate	Solution's Specific Activity	Solution's Specific Activity May 15	Counting Efficiency %
1	9,083	59.6 ± 1.2	3,850	534 ± 5	0.1232	0.638	2.48
2	8,999	69.8 ± 1.3	3,850	467 ± 5	0.1030	0.549	2.14
3	9,426	67.0 ± 1.3	3,850	482 ± 5	0.1078	0.577	2.24
4	9,318	59.4 ± 1.2	3,850	460 ± 5	0.1043	0.562	2.19
5	9,322	65.5 ± 1.0	3,850	485 ± 5	0.1090	0.593	2.31
6	9,049	64.7 ± 1.2	3,850	467 ± 5	0.1043	0.572	2.22
7	9,161	57.8 ± 0.9	3,850	369 ± 4	0.0808	0.444	2.31
8	9,249	61.6 ± 1.2	3,850	385 ± 4	0.0838	0.463	2.40
9	9,114	53.7 ± 1.2	3,850	355 ± 4	0.0783	0.438	2.27
10	8,986	53.6 ± 1.2	3,850	254 ± 3	0.0521	0.293	2.28
11	9,237	62.8 ± 1.2	3,850	257 ± 3	0.0505	0.284	2.21
12	9,026	55.6 ± 1.2	3,850	169 ± 2	0.0293	0.166	2.57

The mean cobalt-60 count rate is computed to be 9,164±42 cpm. The arithmetic mean percent counting efficiency is computed to be (2.30 ±0.04)%. The errors quoted are the standard deviations from the mean values. The errors quoted in the table above are also standard deviations. A plot of the calibration data is shown in Figure 11.

Because the counting system was calibrated in September, 1958, and the final test runs on the centrifugal evaporator were made in March and April, 1959, the question arose as to whether the original calibration had changed during the interval. To investigate this possibility, two counting system calibrations were made on March 21, 1959. A fifty-lambda volume of the February 19, 1959, feed solution was diluted to 1,000 milliliters, and a 250 milliliter and 100 milliliter aliquot of this solution were each taken and diluted to 1,000 milliliters. The specific activities of these solutions were computed to be 20.1 and 8.05 counts per minute per milliliter, respectively, on March 21, 1959. In the first calibration run, 898 milliliters of the 20.1 cpm/ml solution was passed through the (previously calibrated) counting system, giving an increase in the count rate equal to 424±7 cpm. The measured solution specific activity was found to be 0.472 cpm/ml, giving a counting efficiency of 2.35%. In the second calibration run, 897 milliliters of the 8.05 cpm/ml solution was passed through the counting system giving an increase in the counting rate of 202±5 cpm. This corresponds to a measured solution specific activity of 0.225 cpm/ml and a counting efficiency of 2.79%. These points are also shown in Figure 11. From these results, it was concluded that the counting system calibration had not changed measurably during the period of interest.

It was also of interest to determine the fraction of the activity fed to the counting system that was not taken up by the ion exchange bed. To do this, the 898 milliliter residue solution from the first recalibration above was evaporated to dryness, and counted on a planchet on the second shelf of a shielded end-window Geiger counter. This count rate, corrected for background, was found to be 5.8±1.2 cpm. The original activity in the 898 milliliters, corrected for the same Geiger counter geometry, was readily computed, because the fifty-lambda aliquot of the feed solution had been counted on the same shelf in the same counter. The activity of the fifty-lambda aliquot was found to be 3,856 cpm. Thus, the total activity in the 898 milliliters was:

$$3{,}856 \times 0.250 \times 0.898 = 866 \text{ cpm (on second shelf).}$$

Thus, the amount of activity in the feed to the counting system that was not taken up by the resin bed was:

$$5.8 \times 100\%/866 = 0.67\%.$$

This loss corresponded to a feed rate to the counting system of 29 milliliters per minute which was 1.5 times as great as the maximum condensation rate in the evaporator for any run.

VII. DETERMINATION OF SPECIFIC ACTIVITY OF FEED SOLUTION

The strontium-89 employed in this research program was received in two nominal five-millicurie shipments from Oak Ridge National Laboratory. The first shipment was used to prepare the solution used in calibrating the counting system. The second shipment was used to prepare the feed solution used in evaluating the performance of the final modification of the centrifugal evaporator. The packing list for each shipment gave the specific activity (to an accuracy of 10%) and the volume of solution received, from which the total activity was computed. Aliquots of these solutions were also counted in a 4-π counter in order to determine the activity to an accuracy better than 10%. The remainder of this section presents the details of the 4-π counting measurements.

The 4-π counter employed is an instrument from the counting laboratory of Professor W. W. Meinke of the Chemistry Department at the University of Michigan. This counter is based upon a design by C. J. Borkowsky[12], and has been described in detail by K. L. Hall[4]. The counter was operated in the proportional region using pure methane gas, for which a thousand-volt plateau beginning at about 3,400 volts was observed at an input pulse setting of 2.5 millivolts. The counter was operated at 3,800 volts in making the strontium-89 measurements.

A. Activity Measurement of First Shipment (May 15, 1958)

Four 50λ (1λ = 0.001 milliliter) aliquots of feed solution were evaporated to dryness on 1/4 mil teflon films stretched over holes in aluminum cards. A second teflon film was then placed over each of

the first films, sandwiching in the active material to prevent contamination of the counter. To prevent spurious counting, the edges of the films were trimmed smooth and fastened tightly to the aluminum card by means of a light application of silicone grease, and then the film and aluminum around it were sprayed with a thin coat of aquadag to provide a conducting film over the teflon. Each sample was counted three times for two-minute periods, yielding the following results:

Sample A
- Run 1 199,553/2.00 = 99,777 cpm
- Run 2 199,446/2.00 = 99,723 cpm
- Run 3 199,252/2.00 = 99,626 cpm
- Average for Sample A = 99,710 cpm

Sample B
- Run 1 198,756/2.00 = 99,378 cpm
- Run 2 199,019/2.00 = 99,509 cpm
- Run 3 198,620/2.00 = 99,310 cpm
- Average for Sample B = 99,400 cpm

Sample C
- Run 1 196,613/2.00 = 98,307 cpm
- Run 2 197,194/2.00 = 98,597 cpm
- Run 3 196,678/2.00 = 98,339 cpm
- Average for Sample C = 98,410 cpm

Sample D
- Run 1 196,650/2.00 = 98,325 cpm
- Run 2 196,670/2.00 = 98,335 cpm
- Run 3 195,920/2.00 = 97,960 cpm
- Average for Sample D = 98,210 cpm

Background = b = 7,005/80.00 = 87.5 $\pm$ 1.1 cpm

The mean of the four samples is:

$$N = \frac{99,710 + 99,400 + 98,410 + 98,210}{4} = 98,930 \text{ cpm}$$

N - b = 98,840
The coincidence correction = + 1,300
The true count rate, $\overline{N}$ = 100,140

The standard deviation of the mean is computed:

N_i	$\lvert\bar{N} - N_i\rvert$	$(\bar{N} - N_i)^2$
100,920	780	60.84×10^4
100,610	470	22.09×10^4
99,620	520	27.04×10^4
99,420	720	51.84×10^4
		Sum = 161.81×10^4

$$\sigma = \sqrt{\frac{161.8 \times 10^4}{(4)(3)}} = 367$$

$$\% \text{ Std. Dev.} = \frac{367 \times 100\%}{100,140} = 0.37\%$$

The true count rate is thus: $100,140 \pm 0.37\%$ cpm.

The specific activity of the feed solution is:

$$100,140 \text{ cpm}/0.050 \text{ ml} = 2.00 \times 10^6 \text{ cpm/ml}$$

$$2.00 \times 10^6 \frac{\text{counts}}{\text{min ml}} \times \frac{1 \text{ min}}{60 \text{ sec}} \times \frac{1 \text{ curie sec}}{3.7 \times 10^{10} \text{ counts}} = 0.900 \times 10^{-6} \frac{\text{curie}}{\text{ml}}$$

The total activity is:

$$0.900 \times 10^{-6} \times 5,000 = 4.50 \times 10^{-3} \text{ curie} = 4.50 \text{ millicurie.}$$

This value, corrected back to May 15, 1958, is:

$$4.50/0.784 = 5.74 \text{ millicuries.}$$

In converting the measured count rate to activity in curies, the assumption was made that 1 count = 1 disintegration; that is, no beta particles were absorbed by the teflon and graphite. The absorption due to the teflon is computed. The absorption coefficient for the beta particles from strontium-89 has been computed from experimental aluminum absorption data and is found to be: $\mu/\rho = 7.65$ cm^2/gm.

For the teflon, $\rho = 2.3$ gm/cm^3, and thus:

$$\mu \approx 7.65 \times 2.3 = 17.60 \text{ cm}^{-1}$$

The fractional attenuation due to the teflon is:

$$e^{-\mu x} \approx e^{-17.60 \times 0.001 \times 2.54/4} = e^{-0.0111} = 0.989$$

Therefore, the teflon absorbs about 1.1% of the beta particles emitted by the strontium-89. Neglecting the absorption due to the very thin graphite film, the activity corrected for absorption by the teflon is:

$$5.74 \times 1.011 = 5.80 \text{ millicuries.}$$

It is felt that this value is accurate to within 5%.

B. Activity Measurement of Second Shipment (February 19, 1959)

Four 50λ samples were prepared for counting exactly as described in Subsection A. The counting results were:

Sample A
- Run 1 244,971/2.00 = 122,486 cpm
- Run 2 244,697/2.00 = 122,349 cpm
- Run 3 244,391/2.00 = 122,196 cpm
- Average for Sample A = 122,344 cpm

Sample B
- Run 1 240,527/2.00 = 120,264 cpm
- Run 2 238,907/2.00 = 119,454 cpm
- Run 3 239,513/2.00 = 119,754 cpm
- Average for Sample B = 119,824 cpm

Sample C
- Run 1 242,269/2.00 = 121,135 cpm
- Run 2 241,761/2.00 = 120,881 cpm
- Run 3 243,022/2.00 = 121,511 cpm
- Average for Sample C = 121,176 cpm

Sample D
- Run 1 243,335/2.00 = 121,668 cpm
- Run 2 241,047/2.00 = 120,524 cpm
- Run 3 242,045/2.00 = 121,023 cpm
- Average for Sample D = 121,072 cpm

Background = b = 1,887/20.00 = 94.4 ± 2.2 cpm.

The mean of the four samples is:

$$N = \frac{122,344 + 119,824 + 121,176 + 121,072}{4} = 121,100 \text{ cpm.}$$

$$N - b = 121,000$$
The coincidence correction = + 1,960
The true count rate, $\bar{N}$ = 122,960 cpm.

The standard deviation of the mean is computed:

N_i	$\lvert\bar{N} - N_i\rvert$	$(\bar{N} - N_i)^2$
124,240	1,280	1.638×10^6
121,640	1,320	1.742×10^6
123,040	80	negl.
122,930	30	negl.
		Sum = 3.380×10^6

$$\sigma = \sqrt{\frac{338 \times 10^4}{(4)(3)}} = 531$$

$$\% \text{ Std. Dev.} = \frac{531 \times 100\%}{122,960} = 0.43\%$$

The true count rate is thus: 122,960 ± 0.43% cpm.

The specific activity of the feed solution is:

$$122,960 \text{ cpm}/0.050 \text{ ml} = 2.46 \times 10^6 \text{ cpm/ml}$$

$$2.46 \times 10^6 \text{ cpm/ml} \times \frac{1 \text{ min}}{60 \text{ sec}} \times \frac{1 \text{ curie sec}}{3.70 \times 10^{10} \text{ counts}} = 1.108 \times 10^{-6} \frac{\text{curie}}{\text{ml}}$$

The total activity is:

$$1.108 \times 10^{-6} \times 5,000 = 5.54 \times 10^{-3} \text{ curie} = 5.54 \text{ millicuries.}$$

This value, corrected back to February 19, 1959, is:

$$5.54/0.952 = 5.82 \text{ millicuries.}$$

Finally, this value is corrected for absorption by the teflon film:

5.82 x 1.011 = 5.88 millicuries.

It is felt that this value is accurate to within 5%.

VIII. OPERATING PROCEDURE

The procedure for making a test run with the centrifugal evaporator is divided into three parts: the preliminary steps, startup, and the run proper. The preliminary steps are as follows:

1. The electronic components are checked out. The ratemeter and recorder are zeroed, and then the recorder is calibrated against the 7,200 cycle pulse from the ratemeter and the 3,600 cycle pulse from the scaler. The high voltage to the Geiger tube is set at 910 volts, and then the standard cobalt-60 source is lowered into the counter assembly and counted for three minutes (approximately 9,000 counts per minute). If the measured count rate does not differ from the running average value by more than 3%, the Geiger tube is assumed to be operating satisfactorily, and a background count is begun.
2. While the background is being counted, the condenser water is turned on, and four liters of condenser water is passed through the condenser housing and to a waste bottle. For this operation valves J, B and F are opened and valves A, C, D and E are closed.
3. When both the background count (15 - 20 minutes) and the four-liter flush are completed, 250 milliliters of the condenser water is passed from the condenser housing through the counting system to a 250-milliliter volumetric flask. For this operation, valves B, C and E are opened and valves A, D and F are closed. The activity in the 250 milliliters

of water is determined and if it is found to be less than five counts per minute, the equipment is ready for the run. At this point, the run background count is begun.

4. The necessary amount of makeup water is added to the feed bottle from the wash bottle. To do this, valves A and D are opened and valves B, C, E and F are closed. About 800 milliliters of makeup water is required for each run.

The startup procedure is as follows:

1. The condensate system is valved for recycle; to do this, valves B, A and D are opened and valves C, E and F are closed.
2. All flow lines are checked for leakage.
3. The predetermined number of heaters are turned on.
4. When the upper thermometer in the air jacket reaches 150 - 160°F, the evaporator is turned on (2 - 4 minutes after the heaters are turned on).
5. When the upper thermometer in the air jacket reaches 160 - 170°F, the pump is turned on (5 - 8 minutes after the evaporator is turned on).
6. The system is allowed to build up to the predetermined operating conditions. During this time it is necessary to adjust the speed of the evaporator and the feed rate so that they are at the desired levels at the start of the equilibration period. This period begins when condensate begins to flow through the monitor rotameter, and continues for as long as it takes (about 30 minutes) for 300 or more

milliliters of condensate to pass from the condenser. As stated earlier, the evaporator operates on total recycle during this time, so no condensate is lost from the system. At the end of the equilibration period, the run proper is begun after taking the background data from the scaler.

The run procedure is as follows:

1. The condensate flow system is revalved to cause the condensate to flow through the counting system. To do this, valve C is opened and valve A is closed. The zero time is noted on the recorder.
2. During the course of the run such adjustments as are necessary are made in the speed of rotation of the evaporator. The following data are recorded at ten-minute intervals:
   a. Temperature in the top of the air jacket.
   b. Temperature in the bottom of the air jacket.
   c. Temperature in the feed bottle.
   d. Feed rotameter setting.
   e. Monitor rotameter setting.
   f. Strobotac reading.
   g. Current through and voltage across drive motor.
   h. Remarks.
3. At the conclusion of the run, the heaters are turned off. About five minutes later the air jacket temperature has dropped below 200°F, and the pump is turned off. The surge tank is allowed to drain and then valve L is opened. The evaporator is then turned off. A sample of the feed

solution is taken by slightly opening valve H to withdraw the desired volume of the solution (about five milliliters). Two fifty-lambda (0.050 milliliter) samples of the feed solution are evaporated to dryness on aluminum planchets, covered with Scotch tape, and counted in a Geiger tube assembly. Two reference fifty-lambda samples of the original February 19, 1959, feed solution are then counted to determine the specific activity of the feed solution at the end of the given run.

4. About an hour after the end of the run, the condenser housing is cool enough to remove and wash, to prepare it for the next run. It is washed three times with deionized water and then reinstalled.

5. The ion exchange bed is eluted with hydrochloric acid (10%) to prepare it for the next run. About one liter of acid is required for this operation. Then the bed is washed with four liters of deionized, deaerated water to remove all traces of the acid. During this entire operation, the count rate in the bed is recorded continuously to make sure that the bed activity is reduced to less than 60 counts per minute. For both the elution and the washing steps, the valves are arranged as follows: valves A, C and F are opened, and valves B, D and E are closed. Upon completion of the washing operation, the system is ready for the next run. The high voltage to the counter is turned down but not off. The electronic equipment is left on continuously to prevent drift during warmup.

IX. EXPERIMENTAL RESULTS

A series of 31 runs were made with the final modification of the centrifugal evaporator to determine the effect of the angular velocity, ω, and the rate of production of vapor, $\dot{W}$, upon the decontamination factor. In all of the runs, the feed rate to the evaporator was held constant at about 460 milliliters/minute. Thirteen of the runs were made at vaporization rates corresponding to approximately 10 milliliters/minute of condensate and angular velocities ranging from 366 - 1098 RPM. Ten of the runs were made at vaporization rates corresponding to approximately 15 milliliters/minute of condensate and angular velocities ranging from 417 - 1016 RPM. Finally, eight runs were made at vaporization rates corresponding to approximately 19 milliliters/minute and angular velocities ranging from 394 - 1105 RPM. The pertinent data relating to these runs are found in Table II, and the decontamination factors are plotted as a function of the angular velocity in Figures 12, 13 and 14.

The permitted ranges of variation for the rate of vaporization and the angular velocity were dictated by the design and construction of the particular centrifugal evaporator studied. At rates of vaporization corresponding to condensation rates less than 10 milliliters/minute, the time required for a run would increase considerably for two reasons. First, the decrease in condensate rate would require a longer time for condensate passage through the counting system in order to achieve a given statistical accuracy in the counting (see Section V). Second, the decrease in condensate rate would result in an increase in the decontamination factor and a corresponding decrease in the condensate

TABLE II

SUMMARY OF DATA FOR RUNS WITH FINAL MODIFICATION OF EVAPORATOR

Run No.	Date of Run	Net Co-60 Count Rate, cpm.	Background Before 250 ml, cpm.	Background After 250 ml, cpm.	Avg. RPM	Avg. T_{top}, °F	Avg. T_{bot}, °F	Avg. T_{ft}, °F	Avg. Feed Rate, ml/min.	Average Condensate Rate, ml/min.	Specific Activity Feed Soln. cpm/ml.	Specific Activity Condens. cpm/ml.	D.F.
I a	3/ 7/59	8,470 ± 50	57.9 ± 1.9	57.6 ± 1.9	700	237	243	197	469	11.3	3.11×10^6	13.1	2.4×10^5
b	3/ 9/59	8,600 ± 50	50.3 ± 1.8	50.6 ± 1.3	704	236	243	197	491	11.3	3.02×10^6	19.3	1.6×10^5
II a	3/10/59	8,570 ± 50	47.1 ± 1.8	45.0 ± 1.2	810	234	241	197	493	10.5	$3.18 \cdot 10^6$	19.4	1.6×10^5
b	3/11/59	8,440 ± 50	46.7 ± 1.8	46.1 ± 1.8	798	235	240	197	493	11.3	2.84×10^6	15.2	1.9×10^5
III a	3/12/59	8,520 ± 50	50.1 ± 1.9	50.8 ± 1.9	909	234	239	194	463	9.8	3.03×10^6	7.68	3.9×10^5
b	3/13/59	8,370 ± 50	44.5 ± 1.5	45.0 ± 1.5	905	234	240	198	493	10.2	2.74×10^6	7.77	3.5×10^5
IV a	3/14/59	8,620 ± 50	44.3 ± 1.5	43.4 ± 1.5	1013	234	240	194	463	8.8	2.83×10^6	4.94	5.7×10^5
b	3/16/59	8,340 ± 50	44.1 ± 1.5	44.2 ± 1.5	993	234	240	196	451	8.8	2.81×10^6	4.46	6.3×10^5
V	3/17/59	8,360 ± 50	39.6 ± 1.7	42.0 ± 1.7	895	248	267	191	439	18.9	2.32×10^6	36.0	6.5×10^4
VI	3/18/59	8,740 ± 50	38.5 ± 1.4	42.3 ± 1.3	756	247	267	195	466	18.9	2.34×10^6	48.1	4.9×10^4
VII	3/19/59	8,620 ± 50	39.5 ± 1.4	40.0 ± 1.3	1105	249	266	193	442	18.0	2.40×10^6	20.0	1.20×10^5
VIII	3/19/59	8,640 ± 50	44.4 ± 1.7	43.2 ± 1.5	1003	247	267	194	466	18.0	2.20×10^6	34.2	6.4×10^4
IX	3/20/59	8,420 ± 50	48.3 ± 1.8	48.3 ± 1.8	1098	237	240	193	419	7.9	2.39×10^6	4.92	$.9 \times 10^5$
X	3/23/59	8,470 ± 50	54.5 ± 1.9	52.2 ± 1.9	592	235	240	198	481	11.3	2.10×10^6	17.72	1.2×10^5
XI	3/24/59	8,500 ± 50	42.3 ± 1.7	45.4 ± 1.7	458	240	242	197	484	11.3	1.98×10^6	24.9	7.9×10^4
XII	3/24/59	8,520 ± 50	44.9 ± 1.7	45.5 ± 1.2	366	245	243	198	474	13.0	2.17×10^6	22.9	9.5×10^4
XIII	4/ 1/59	8,580 ± 50	49.3 ± 1.6	48.5 ± 1.6	632	236	239	195	464	11.3	1.87×10^6	10.4	1.80×10^5
XIV	4/ 2/59	8,510 ± 50	52.7 ± 1.6	48.3 ± 1.1	621	246	249	194	464	15.0	1.54×10^6	31.2	4.9×10^4
XV	4/ 3/59	8,620 ± 50	58.4 ± 2.0	60.6 ± 1.4	725	244	249	194	463	15.1	1.45×10^6	26.0	5.6×10^4
XVI	4/ 4/59	8,630 ± 50	47.1 ± 1.5	48.5 ± 1.6	823	245	251	194	452	14.7	1.43×10^6	11.4	1.3×10^5
XVII	4/ 4/59	8,590 ± 50	47.3 ± 1.5	45.7 ± 1.5	915	243	250	194	478	14.7	1.24×10^6	17.1	7.3×10^4
XVIII	4/ 6/59	8,550 ± 50	45.7 ± 1.7	47.0 ± 1.5	1016	242	251	194	466	14.7	1.19×10^6	6.38	1.9×10^5
XIX	4/ 7/59	8,680 ± 50	45.8 ± 1.7	43.6 ± 1.5	802	245	251	196	464	16.2	1.12×10^6	25.1	4.5×10^4
XX	4/ 8/59	8,440 ± 50	48.6 ± 1.6	47.2 ± 1.4	506	243	247	196	463	15.4	0.990×10^6	36.2	2.7×10^4
XXI	4/ 8/59	8,550 ± 50	56.1 ± 1.7	54.8 ± 1.7	417	245	248	197	469	15.4	1.12×10^6	20.4	5.5×10^4
XXII	4/ 9/59	8,410 ± 50	50.5 ± 1.6	51.8 ± 1.6	757	243	247	194	469	15.4	0.880×10^6	4.88	1.8×10^5
XXIII	4/10/59	8,440 ± 50	41.5 ± 1.4	43.9 ± 1.0	768	241	246	197	457	15.4	0.786×10^6	6.04	1.3×10^5
XXIV	4/11/59	8,580 ± 50	46.0 ± 1.5	45.2 ± 1.5	631	248	265	194	454	19.8	0.766×10^6	42.3	1.8×10^4
XXV	4/14/59	8,560 ± 50	47.5 ± 1.5	45.9 ± 1.2	511	244	261	197	454	20.2	1.05×10^6	36.2	2.9×10^4
XXVI	4/14/59	8,610 ± 50	48.8 ± 1.5	49.8 ± 1.3	394	248	263	194	448	20.2	1.10×10^6	62.3	1.8×10^4
XXVII	4/15/59	8,560 ± 50	56.1 ± 1.9	57.8 ± 1.2	789	245	265	196	457	20.2	0.805×10^6	7.80	1.0×10^5

specific activity. This effect would further increase the time required to achieve the desired statistical accuracy in counting. It was not felt that the design of this machine was such that it could be operated for extended periods of time. In order to attain rates of vaporization corresponding to more than 20 milliliters/minute of condensate, it would be necessary to heat the evaporator to temperatures where trouble might well be encountered. The most obvious example of such trouble is the failure of the Permatex Gasket Cement used to seal the heads to the body of the evaporator, which would result in leakage of the feed solution from the evaporator. At speeds below about 350 RPM, the accuracy of speed control of the evaporator fell off markedly due to the characteristics of the drive motor employed, and thus, all data were taken at greater speeds. At speeds above 1100 RPM, the evaporator began to vibrate due to dynamic unbalance, and rather than attempt to interpret the effect of the vibration upon the decontamination mechanism, data were not taken above this speed.

An examination of Figures 12, 13 and 14 shows that a considerable amount of scatter exists in the decontamination factor measurements. This scatter is also characteristic of decontamination studies made with conventional evaporators treating radioactive solutions.[6] Its exact cause is obscure, but is related to random surges of entrainment in the vapor stream. An increase in the vapor velocity would appear to increase the amount of entrainment produced by such a surge, and thus, increase the scatter. A comparison of Figures 12 and 13 tends to confirm this conclusion. To reduce the scatter, it would seem necessary to either reduce the rate of production of vapor, or else operate for times long

enough to smooth out the surge effects upon the data. The latter point was inapplicable to this study, both because of the inherently long time required and the relatively low capacity of the counting system employed. There are two other probable contributions to the scatter observed in the data obtained in this research program. First, the inner surface of the evaporator is slightly out of round (as determined in a static balancing test) which gives rise to areas where the liquid film thickness varies in a transient manner. In areas where the film does become thinner than the average thickness, an increase in bubble formation, and consequently, entrainment occurs. Second, the decontamination factor is quite sensitive to the rate of vaporization, which varied somewhat from run to run within a given series due to variation in the ambient temperature.

An examination of Figure 12 shows that the logarithm of the decontamination factor is approximately linear in the evaporator angular velocity at an average condensate rate of 10.4 milliliters/minute. If it is assumed that this linearity is exact for all three vaporization rates studied, then it becomes possible to determine the values of α and β in:

$$D.F. = \alpha e^{\beta \omega},$$

for each of the vaporization rates by a least-squares fit of the data. Also, if this linearity is exact, then the decontamination model evolved in Section II is exact, and it can be used to evaluate the most probable diameter of a droplet undergoing entrainment, as well as the distribution-in-diameter of the entrained droplet current from the experimental

data. This is done as follows:

$$\ln(D.F.) = \ln\alpha + \beta\omega,$$

$$\log(D.F.) = \log\alpha + 0.434\beta,$$

Set: $\log(D.F.) = Y,\ \log\alpha = b,\ 0.434\beta = m,\ \omega = X.$

Then:

$$b = \frac{\sum X_i^2 \sum Y_i - \sum X_i \sum X_i Y_i}{n\sum X_i^2 - (\sum X_i)^2},$$

$$m = \frac{n\sum X_i Y_i - \sum X_i \sum Y_i}{n\sum X_i^2 - (\sum X_i)^2},$$

where n is the total number of points being fitted in a given series. The dashed lines in Figures 12, 13 and 14 correspond to the least-squares fit of the data. Table III below is a summary of the results of these calculations.

TABLE III

SEMILOGARITHMIC LEAST-SQUARES FIT OF THE EXPERIMENTAL DATA

$\dot{W}$ ml/min	b	m, sec.	α	β, sec.	N_o Number / ft^2 sec ft	D_o feet
10.4	4.393	1.20×10^{-2}	2.47×10^{4}	2.77×10^{-2}	0.898×10^{-15}	0.951×10^{-6}
15.2	4.145	0.963×10^{-2}	1.395×10^{4}	2.22×10^{-2}	2.26×10^{-15}	0.924×10^{-6}
19.3	3.808	1.09×10^{-2}	0.642×10^{4}	2.50×10^{-2}	7.89×10^{-15}	1.17×10^{-6}

It is seen that within the experimental error, the most probable diameter of an entrained droplet is constant over the range of

vaporization rates studied. The reason for this is that the force tending to eject droplets into the vapor depends primarily upon the surface tension of the liquid, which in turn, depends only upon the temperature of the liquid at its free surface. Since the evaporator was operated at essentially atmospheric pressure at all times, the temperature at the free surface of the liquid film was constant, and thus, it would be expected that the most probable droplet diameter would remain constant. The most probable diameter of a droplet of 1×10^{-6} foot corresponds to approximately 10 microns. This value is reasonable since the range of droplet diameters in conventional evaporator vapor streams has been found to extend from submicron to greater than 100 micron values.(8)

It is also seen that the parameter N_o, which is proportional to the total droplet current moving with the vapor, increases in a greater than linear manner with increasing $\dot{W}$, over the range of $\dot{W}$ investigated. To appreciate the mathematical cause for this, it is necessary to consider the equation for N_o:

$$N_o = \frac{15 D_o \dot{W}}{\pi^2 r_2 L \rho_l \alpha}.$$

If N_o were linear in $\dot{W}$, then α, the decontamination factor at zero RPM, would have to remain constant with increasing $\dot{W}$. But a decrease in α with increasing $\dot{W}$ is anticipated, since it is to be expected that the agitation at the free surface of the liquid film increases with increasing $\dot{W}$, especially at zero RPM. Physically, this greater than linear increase of N_o with $\dot{W}$ is because increasing $\dot{W}$ simultaneously increases both the total rate of production of droplets of all diameters and the range of diameters of entrained droplets.

It was not possible to test the criterion derived in Section II for the transition from nucleate to surface evaporation. This point is considered further in Section X following.

X. CONCLUSIONS

This research program has investigated the effect of centrifugal force upon the decontamination factor achieved in a centrifugal evaporator at angular velocities up to 1100 RPM, and for vapor production rates corresponding up to 19.3 milliliters per minute of condensate. The maximum decontamination factor measured in this range of conditions was 6.3×10^5. Based upon the assumption of evaporation by a nucleate mechanism, a model for the de-entrainment of liquid droplets from the vapor stream has been developed and tested successfully. It is reasonable to ask if this model predicts that the decontamination factor will continue to rise exponentially with the evaporator angular velocity at a given vaporization rate for angular velocities greater than 1100 RPM. As long as vaporization occurs by the nucleate mechanism, this exponential relationship should continue to hold. However, for a given rate of vaporization, an evaporator angular velocity should be attained at which the evaporation mechanism shifts from the nucleate to the surface type. At this or greater angular velocities, no bubble formation should occur in the liquid film flowing down the inner wall of the evaporator, and a significant improvement in the decontamination factor should thus be realized. This concept is studied quantitatively in Section II where the criterion for the shift from the nucleate to the surface evaporation mechanism is derived. This criterion is:

$$q \leq \frac{AKa}{g_c} \omega^2 \left(\frac{2\pi}{60}\right)^2.$$

The various terms comprising this inequality are defined in Section II. For the particular centrifugal evaporator studied, this expression reduces to:

$$q \leq 1.622 \times 10^{-4} \omega^2.$$

If the minimum vaporization rate corresponds to a rate of condensation of 10.4 milliliters per minute, then:

$$q = 10.4 \times (1/4 - 4) \times 60 \times 970 = 1,333 \text{ Btu/hr}$$

and

$$\omega \geq \sqrt{\frac{1.333 \times 10^3}{1.622 \times 10^{-4}}} = 2,870 \text{ RPM},$$

although this value is an upper limit, as explained in Section II. From this it is seen that in order to shift the vaporization mechanism from the nucleate to the surface type, it is necessary to drive the evaporator at speeds considerably above the upper limit found feasible for the model constructed and studied.

In conclusion, it is seen that at relatively low angular velocities the decontamination mechanism in the centrifugal evaporator corresponds to the de-entrainment from the vapor stream of liquid droplets produced by bubbles of vapor spattering at the free surface of the liquid film. Increasing the angular velocity of the evaporator causes an exponential increase in the decontamination factor probably up to the point where the vaporization mechanism shifts from the nucleate to the surface type. At this point and beyond, the decontamination mechanism is probably just the complete supression of bubble formation in the liquid film, and the consequent elimination of droplet injection into the vapor stream. In the experimental program reported in this thesis,

the point of shift of the vaporization mechanism was never attained due to the inability to reach the necessary evaporator speeds.

If it is desired to employ a centrifugal evaporator to achieve decontamination factors of 10^7 or better on a commercial basis, where high vaporization rates are encountered, the machine would have to be designed to operate at quite high speeds. It must be realized, however, that operation at considerably higher speeds may introduce new problems that will require experimental study. For example, if the lateral wall of the evaporator is out of round, regions of reduced liquid film thickness occur, and nucleate evaporation with its associated droplet production may take place. Significantly, the film thickness at a point closer to the axis of rotation decreases with increasing angular velocity. Another problem that might arise at higher speeds is related to the increase in vibration of the evaporator due to dynamic unbalance. This problem is the agitation of the surface of the liquid film in such a manner that droplets are ejected into the vapor by a wave action at the surface.

Finally, an experimental program investigating the exact nature of the decontamination mechanism at high rotational speeds would certainly prove fruitful in augmenting the information obtained from the present program. It might also have as one of its aims, the evaluation of the centrifugal evaporator as a commercially feasible machine for concentrating radioactive solutions, since if such feasibility exists, it almost certainly will be found at high evaporator rotational speeds, as stated earlier. For this machine to be commercially feasible, it would have to compete favorably with conventional evaporators in which a fiberglass

filter column is employed to remove entrained droplets of the feed solution, and with which decontamination factors of better than 10^7 are attainable.

A valuable byproduct of this research program was the successful development of a counting system for determining the specific activity of very dilute (10^{-15} curies/milliliter) aqueous solutions containing energetic beta-emitting isotopes. This counting system was found to operate completely satisfactorily in the seven-month period during which it was employed in this research. In this period, it was used 56 times. Besides its accuracy and reliability, the counting system is of a rather simple design, and is inexpensive to construct. Its primary disadvantage lies in the necessity for chemical treatment at the beginning of a specific activity determination to remove the activity deposited in the previous run.

FIGURES 1 - 14

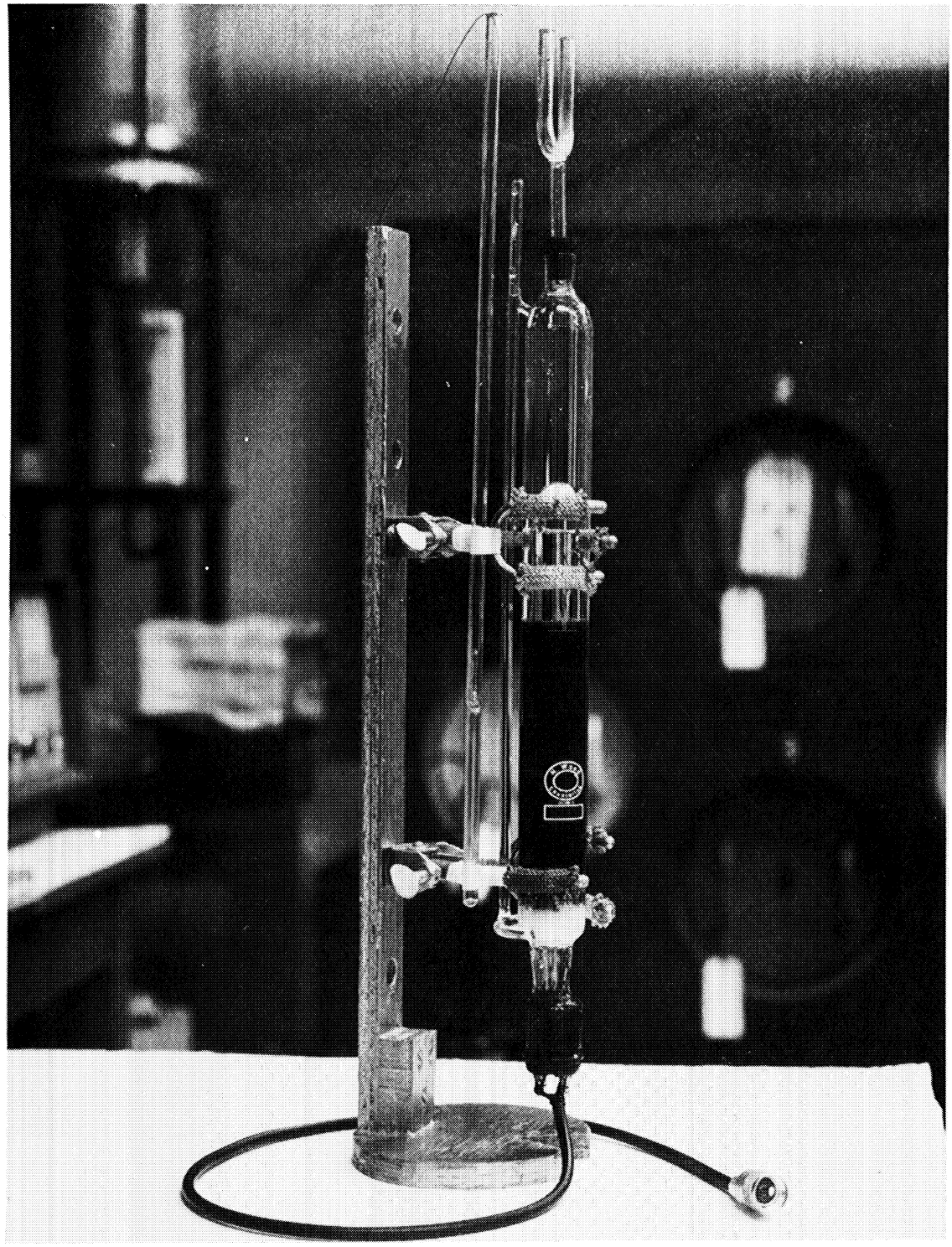

Figure 1. Picture of Counting System

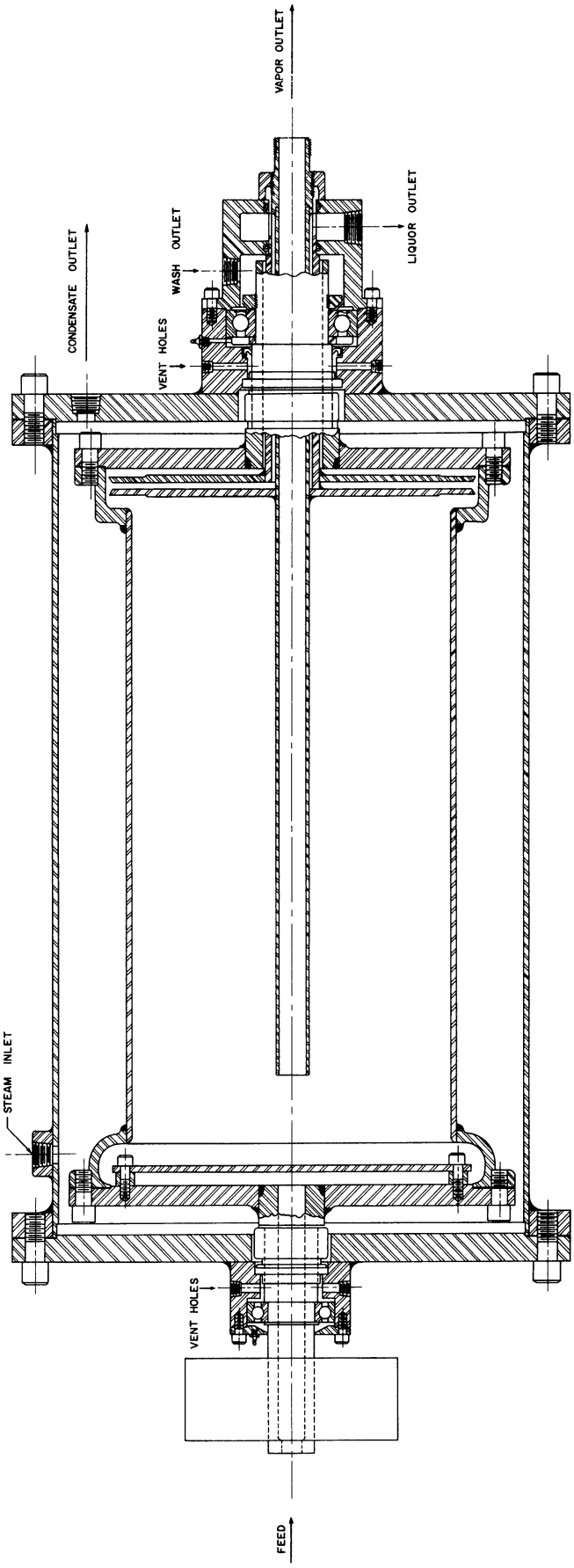

Figure 2. Drawing of Prototype Evaporator

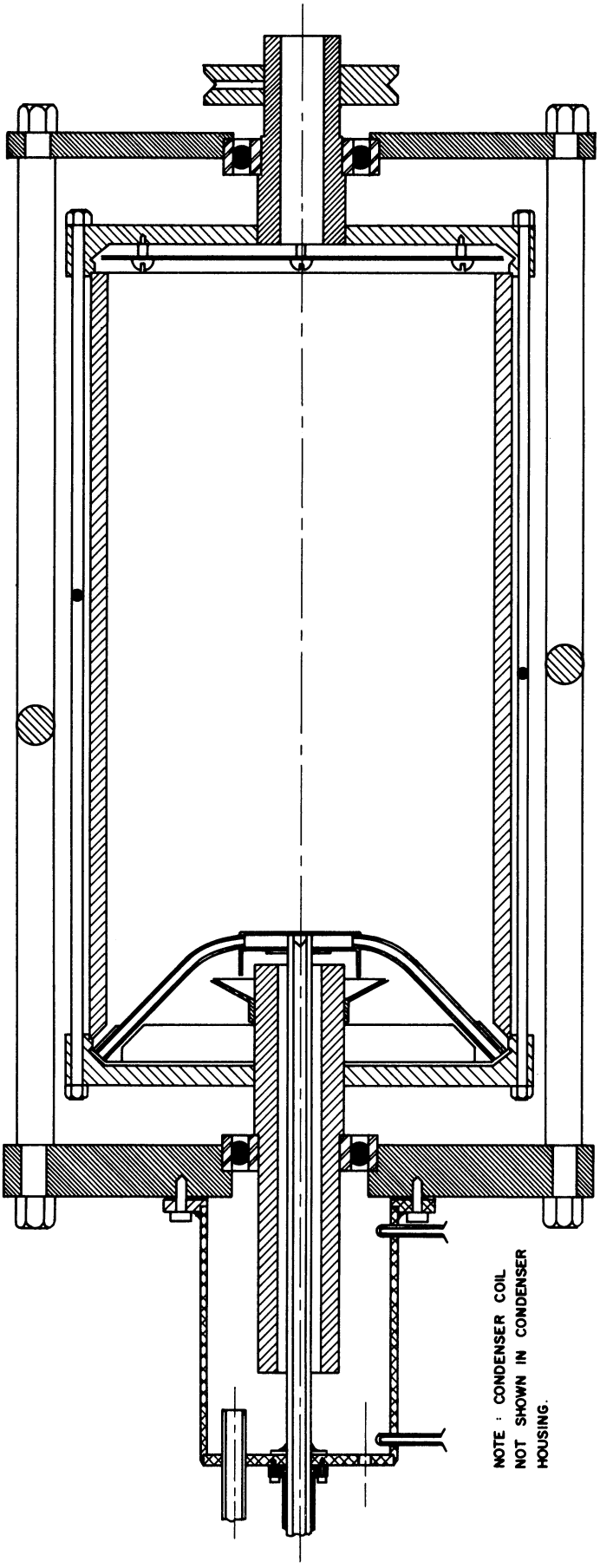

Figure 3. Drawing of First Modification of Evaporator

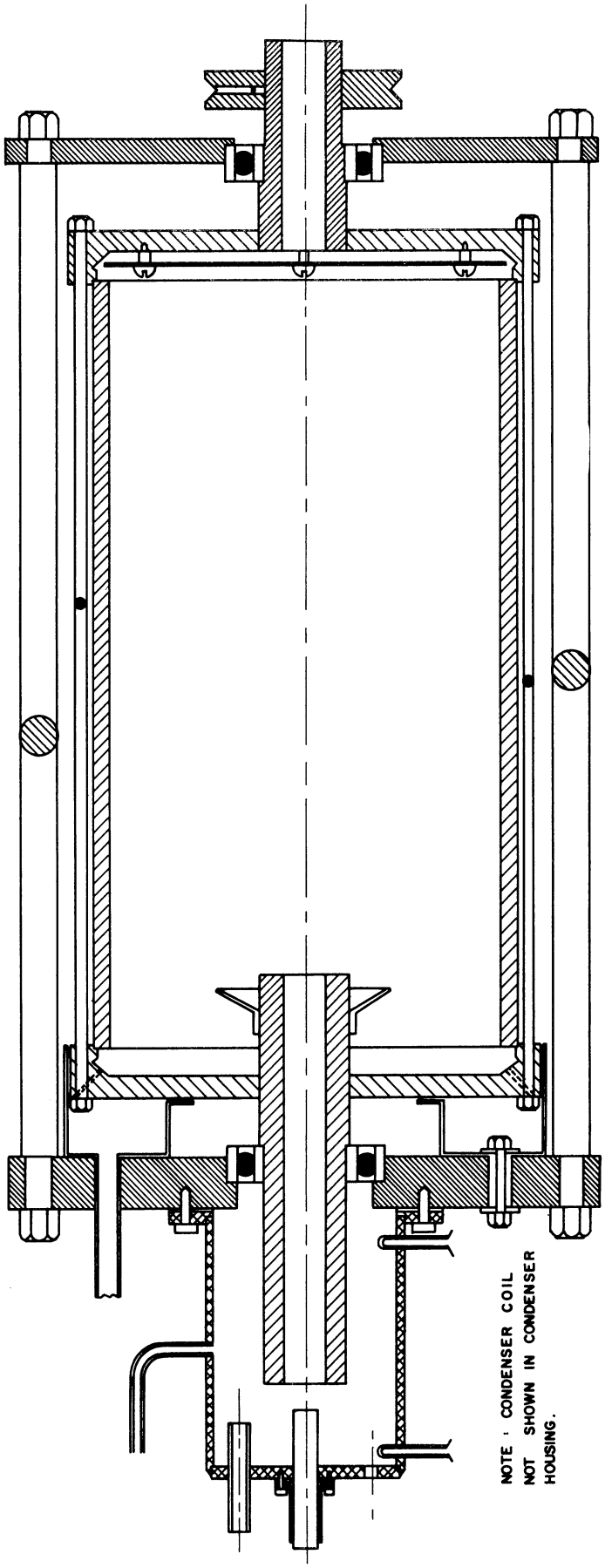

Figure 4. Drawing of Second Modification of Evaporator

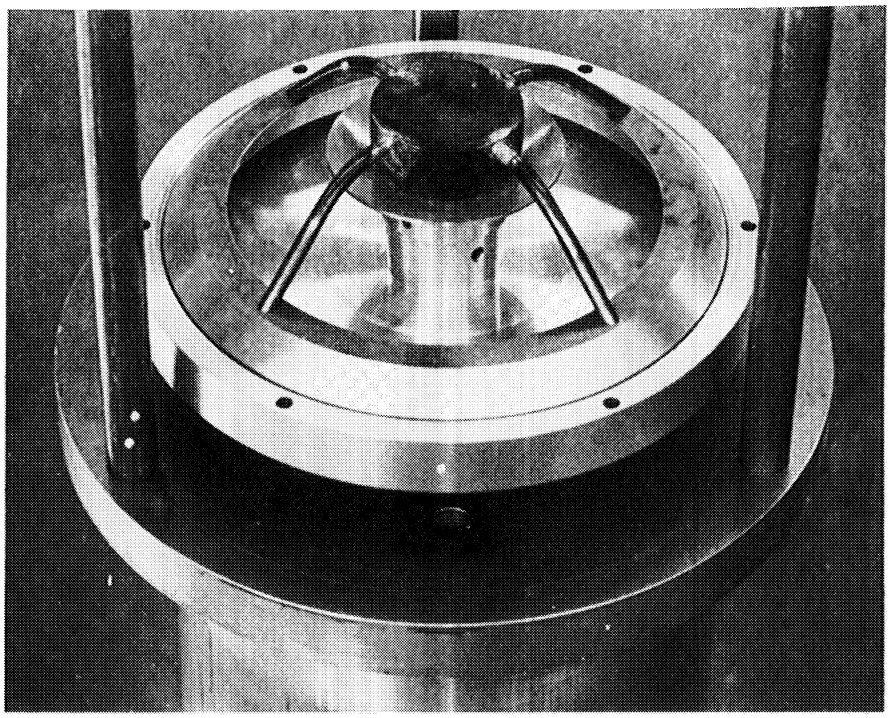

Figure 5. Picture of Lower Head and Stator in First Modification

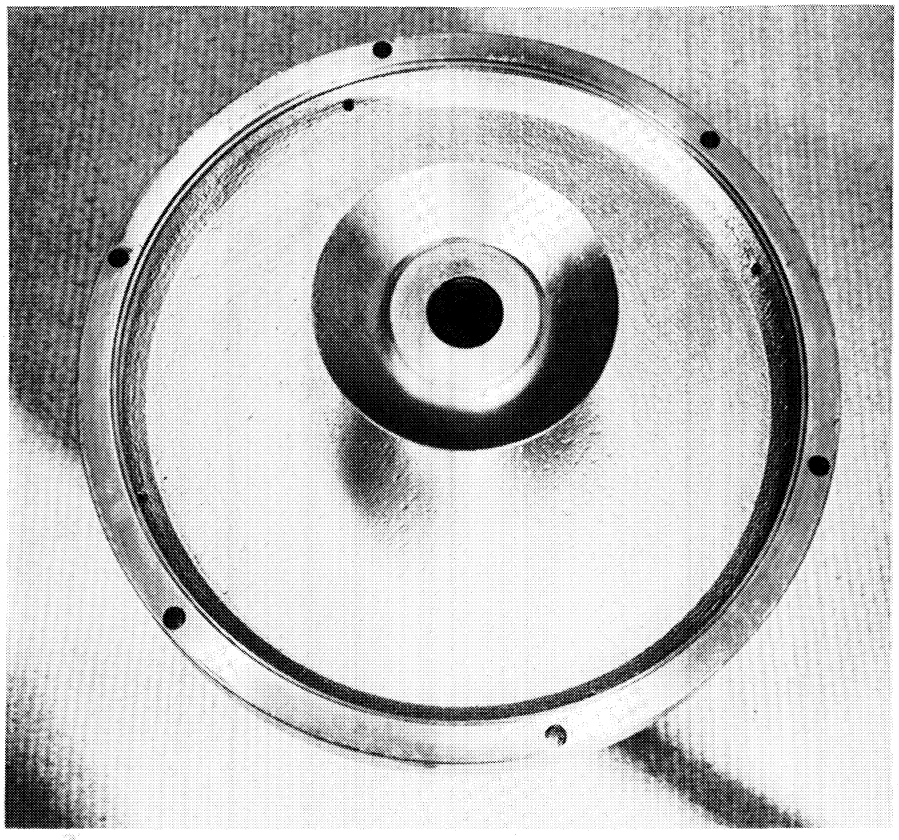

Figure 6. Picture of Lower Head and Egress Holes in Second Modification

Figure 7. Picture of Condenser Housing

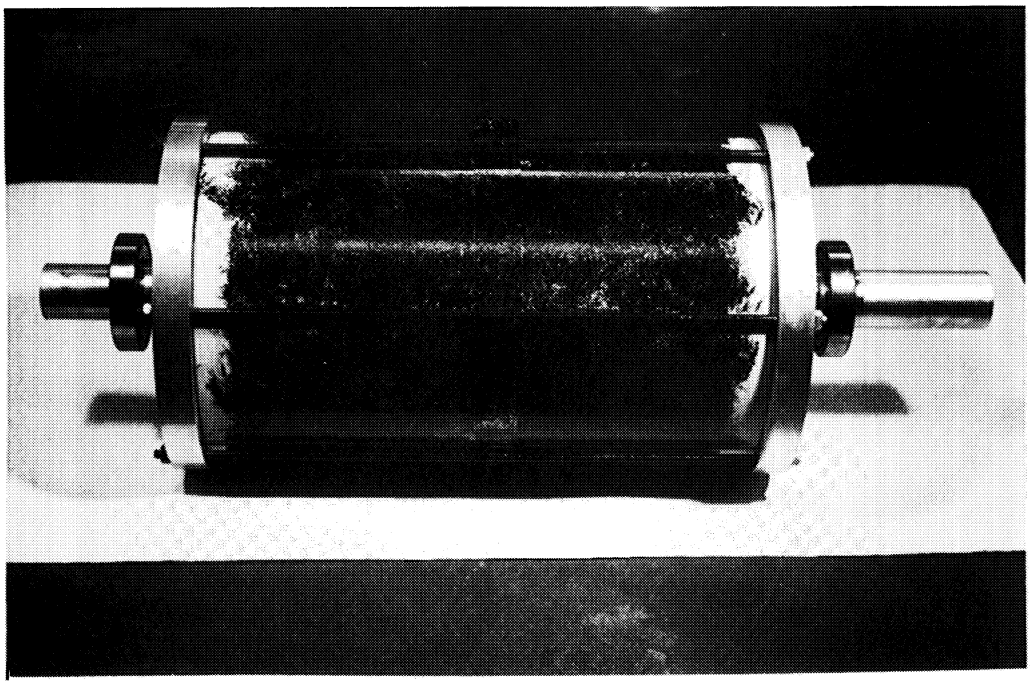

Figure 8. Picture of Final Modification of Evaporator Body

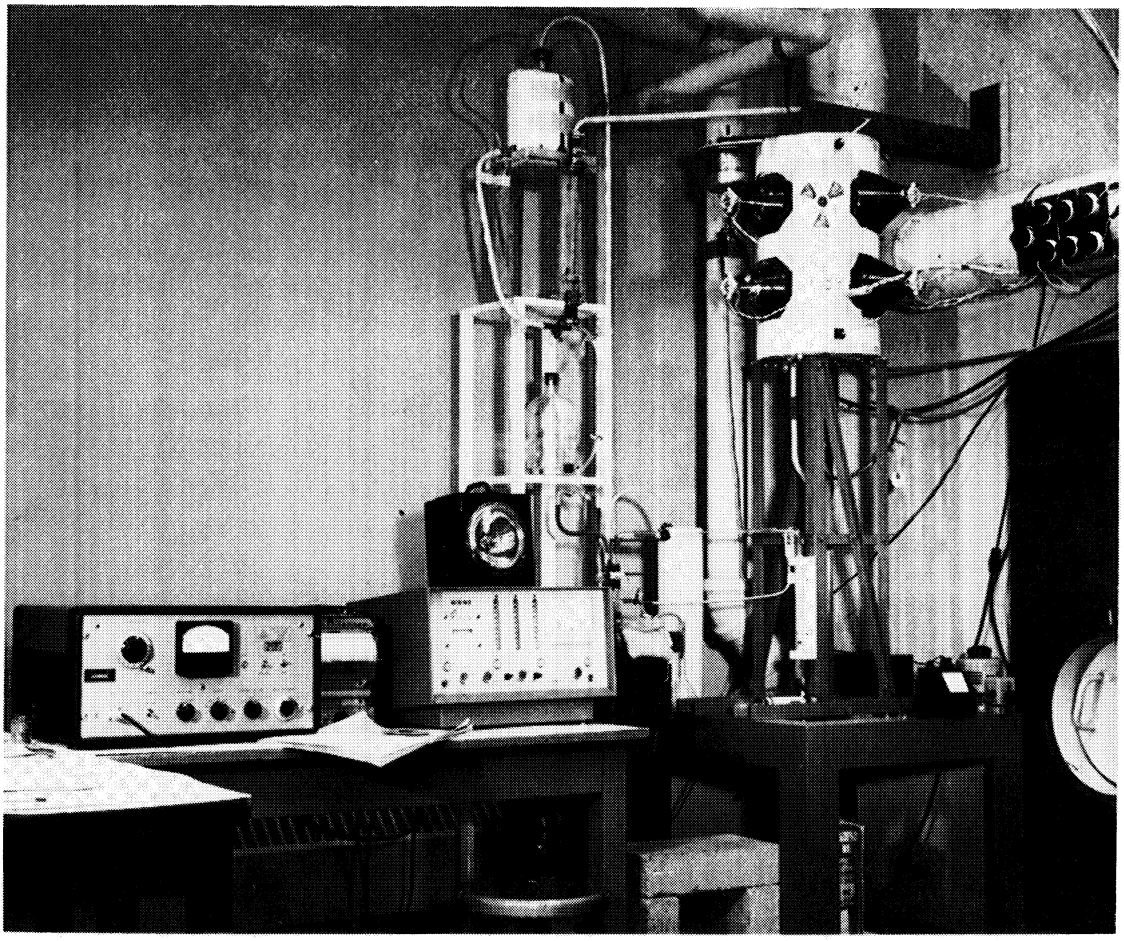

Figure 9. Picture of Entire Apparatus

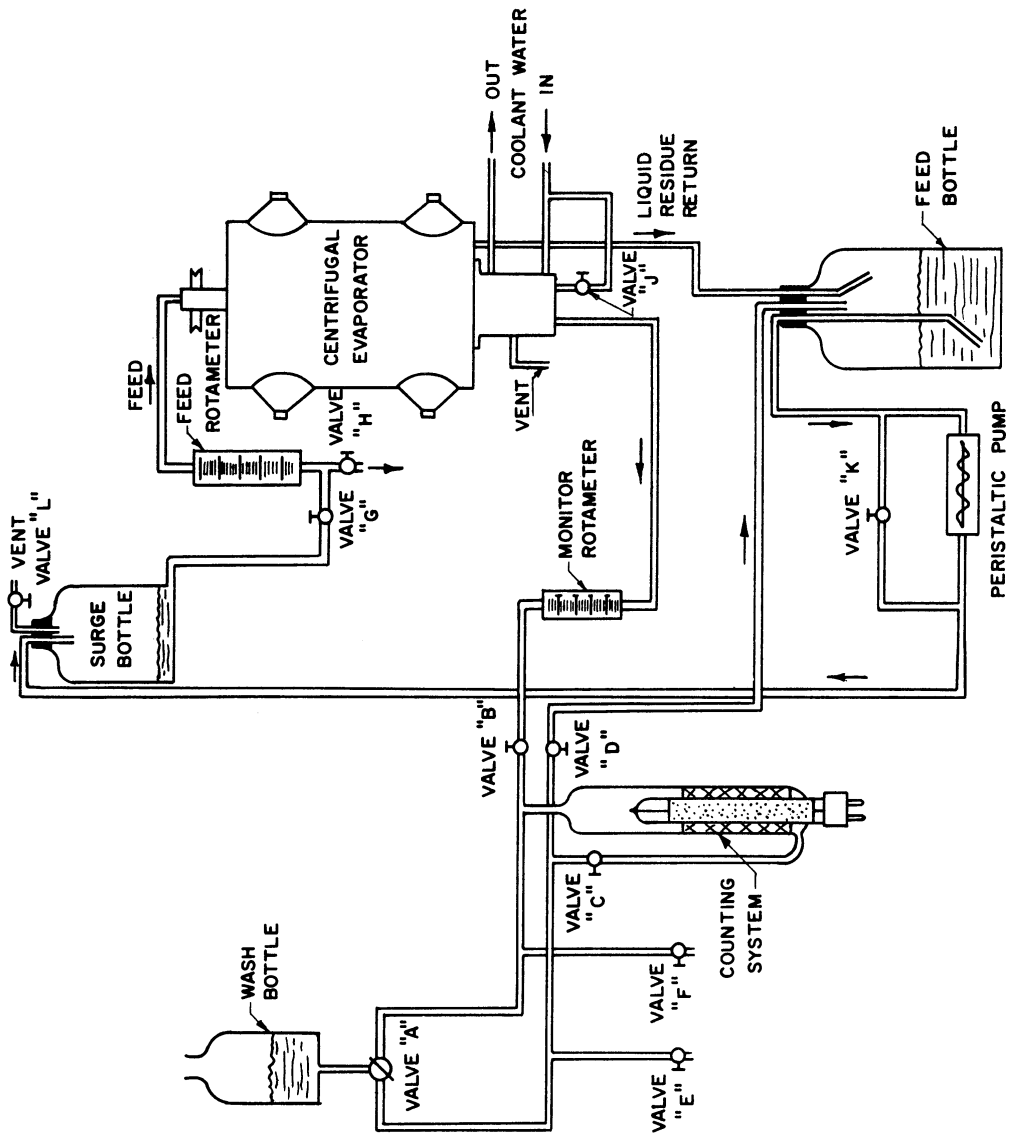

Figure 10. Schematic Flow Diagram of Apparatus

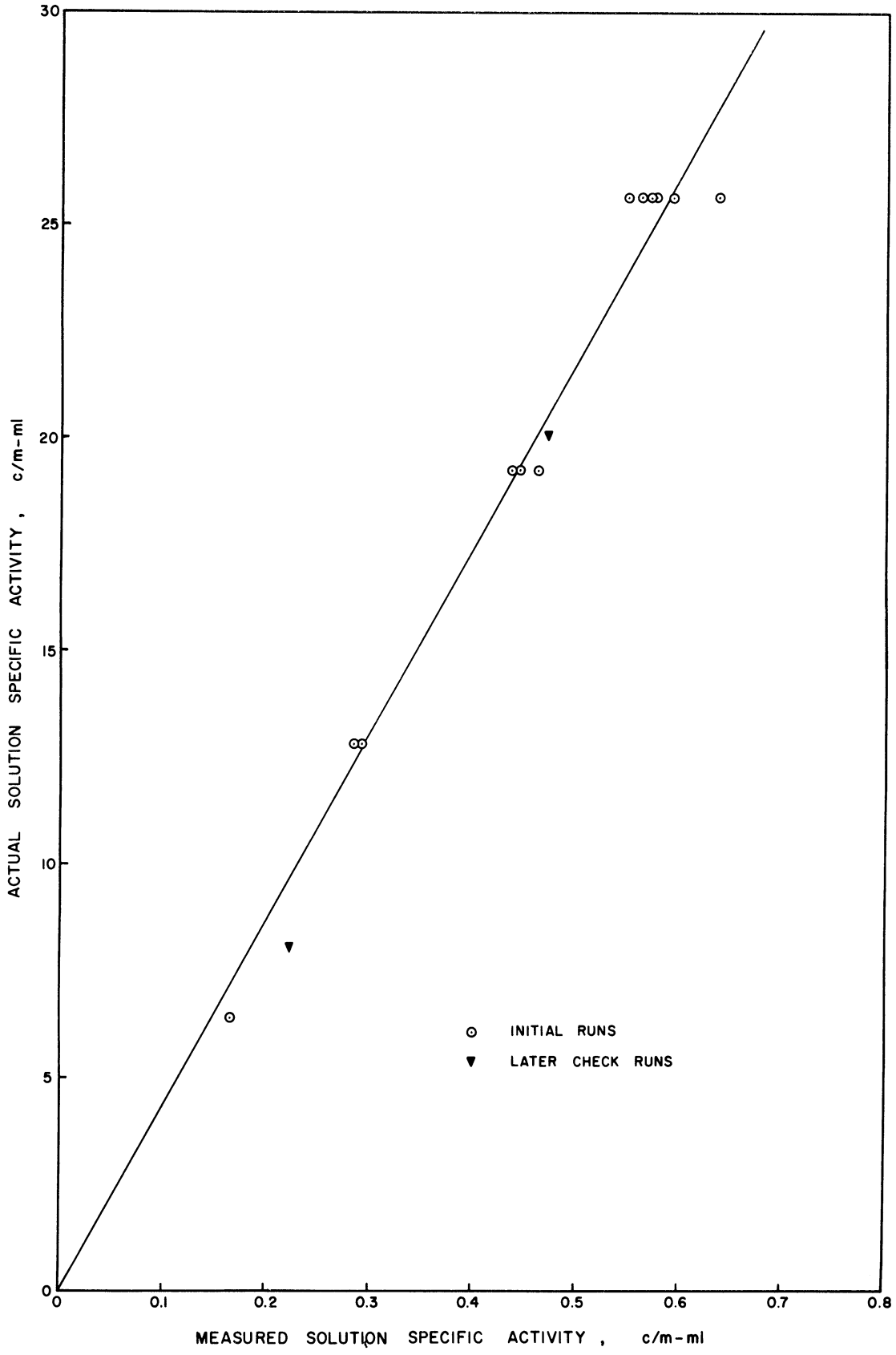

Figure 11. Calibration Curve for Counting System

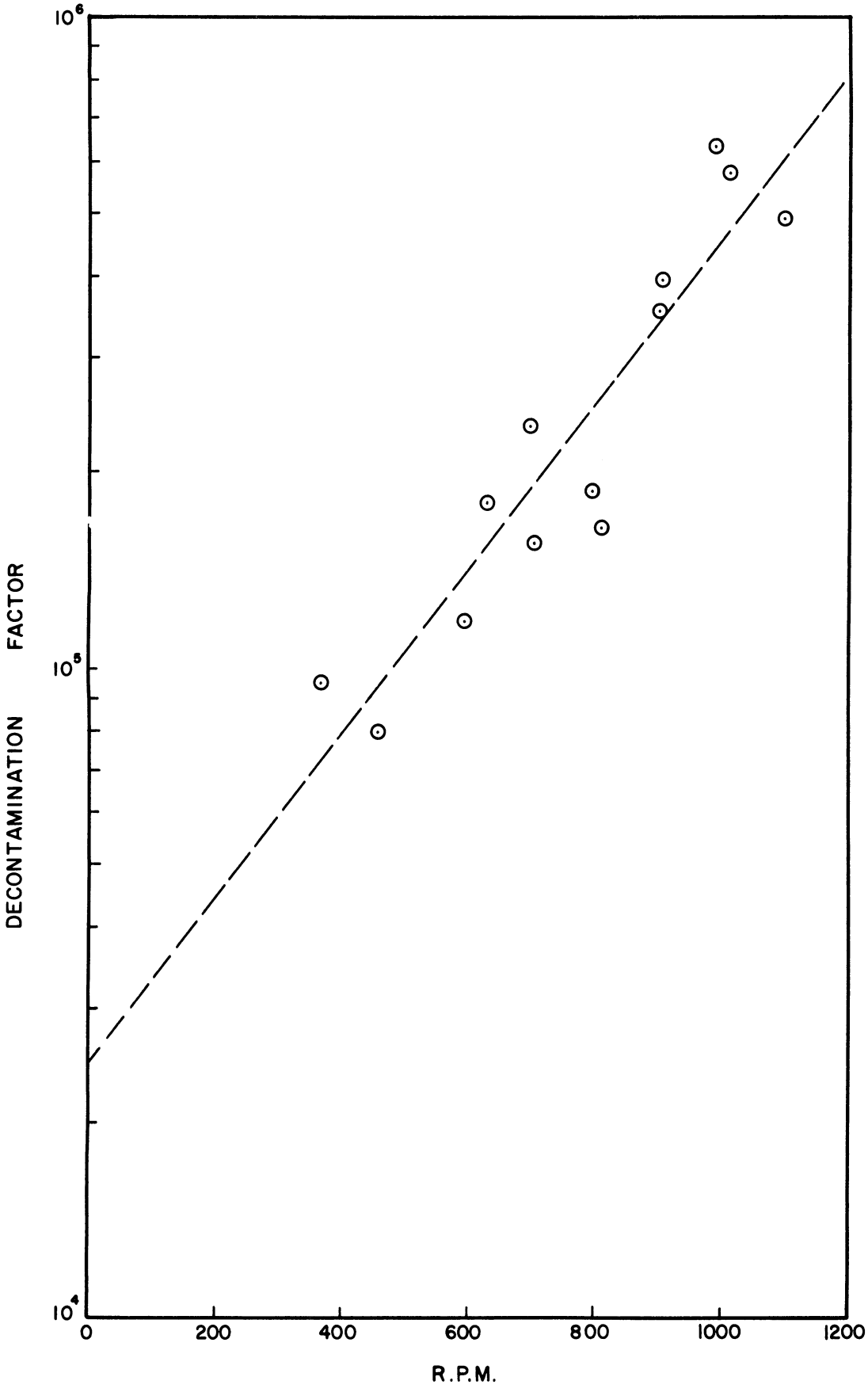

Figure 12. Plot of Decontamination Factor vs. RPM for $\dot{W}$ = 10.4 ml/min.

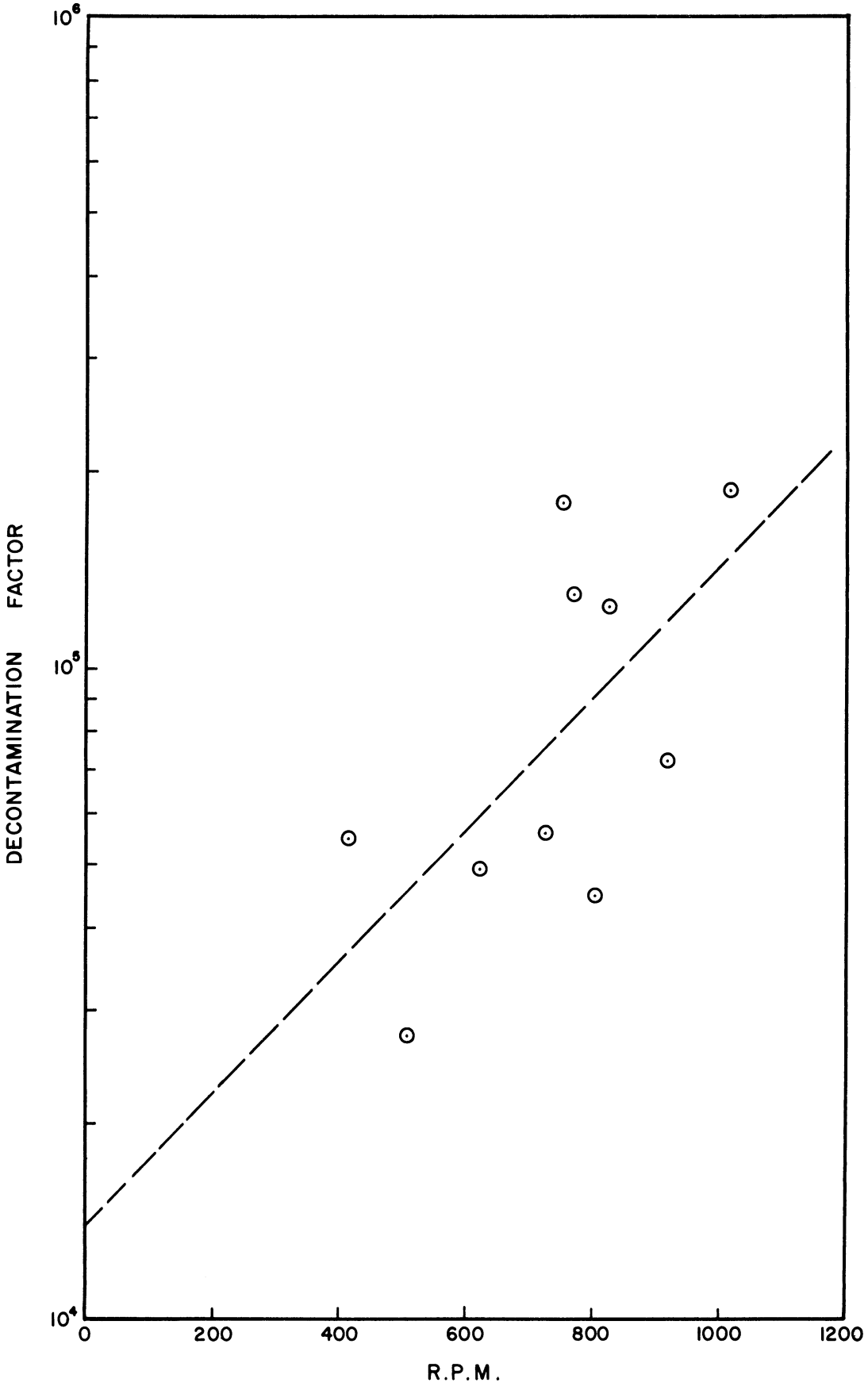

Figure 13. Plot of Decontamination Factor vs. RPM for $\dot{W}$ = 15.2 ml/min.

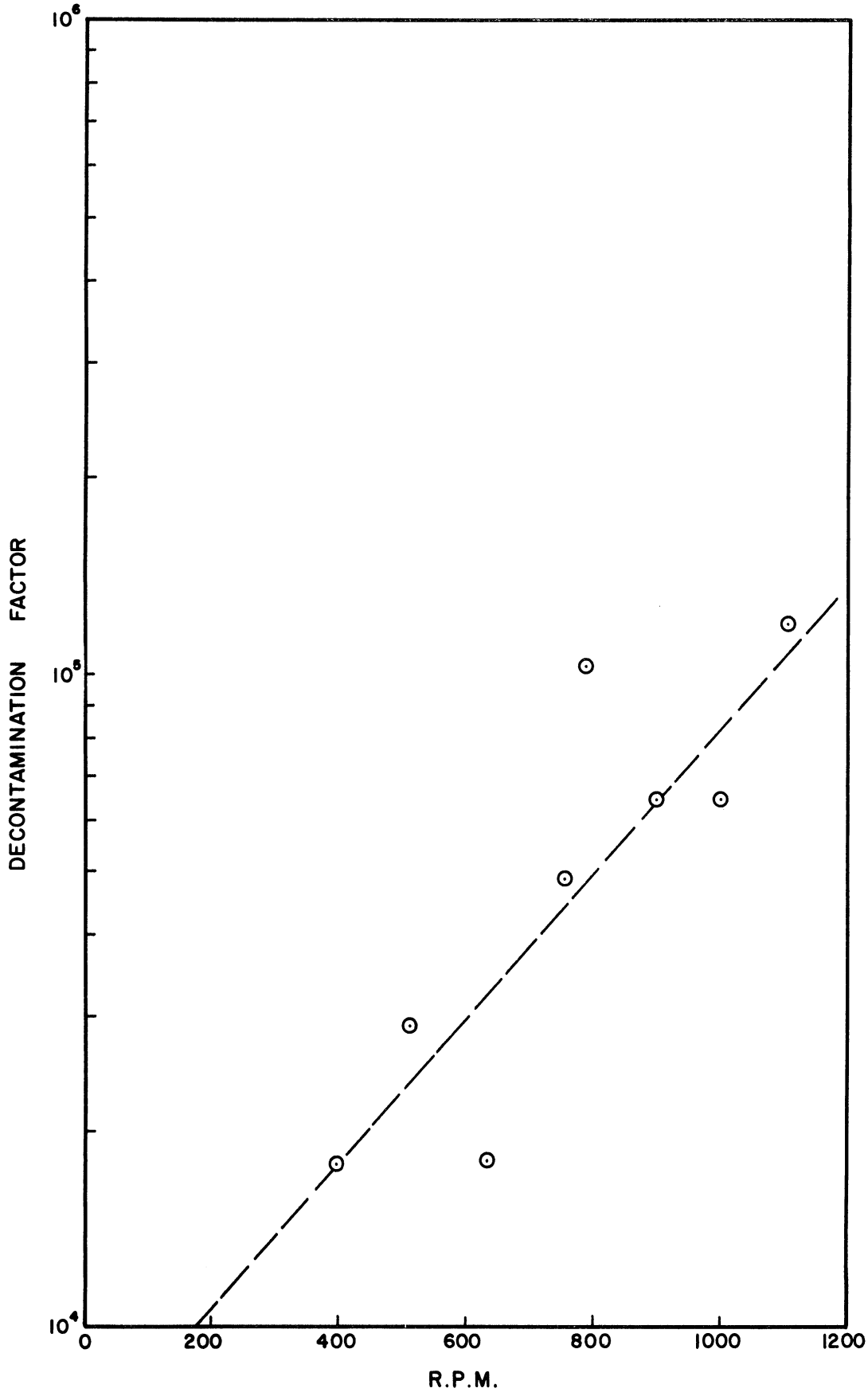

Figure 14. Plot of Decontamination Factor vs. RPM for $\dot{W}$ = 19.3 ml/min.

APPENDIX A

CALCULATION OF EFFECT UPON DECONTAMINATION FACTOR OF INJECTING ACTIVE LIQUID INTO INACTIVE SATURATED VAPOR

In this section, a calculation is made to show the reduction in the decontamination factor that occurs when one drop (0.050 ml) of active liquid is injected into 100 liters of the previously inactive vapor.

Let: v_l = specific volume of saturated liquid at 212°F (0.01672 ft^3/lb).

v_g = specific volume of saturated vapor at 212°F (26.80 ft^3/lb).

s_l = initial specific activity of liquid, curie/lb.

s_g^o = initial specific activity of vapor, curie/lb.

D_o = initial decontamination factor of vapor (here taken as 10^7).

D_f = final decontamination factor of vapor.

S_g = final specific activity of vapor, curie/lb.

V_l = volume liquid injected into vapor = 0.050 ml = 1.767×10^{-6} ft^3.

V_g = volume of vapor = 100 liters = 3.535 ft^3.

An activity balance gives:

$$\frac{V_l}{v_l} S_l + \frac{V_l}{v_g} \times 10^{-7} S_l = \left(\frac{V_l}{v_l} + \frac{V_l}{v_g}\right) S_g \qquad \text{Note: } S_g^o \equiv S_l D_o^{-1}$$

$$S_l \left(\frac{V_l}{v_l} + \frac{V_g}{v_g} \times 10^{-7}\right) = S_g \left(\frac{V_l}{v_l} + \frac{V_g}{v_g}\right).$$

$$D_f \equiv \frac{S_\ell}{S_g} = \frac{\frac{V_\ell}{V_\ell} + \frac{V_g}{V_g}}{\frac{V_\ell}{V_\ell} + \frac{V_g}{V_g} \times 10^{-7}} = \frac{\frac{1.767 \times 10^{-6}}{1.62 \times 10^{-2}} + \frac{3.535}{26.80}}{\frac{1.767 \times 10^{-6}}{1.62 \times 10^{-2}} + \frac{3.535 \times 10^{-7}}{26.80}}$$

$$= 1.21 \times 10^{3}.$$

Thus, by injecting one drop of active liquid into 100 liters of formerly inactive vapor, the decontamination factor of the latter is decreased to 10^3.

APPENDIX B

DERIVATION OF EQUATION FOR CENTRIFUGAL PRESSURE IN LIQUID FILM IN EVAPORATOR

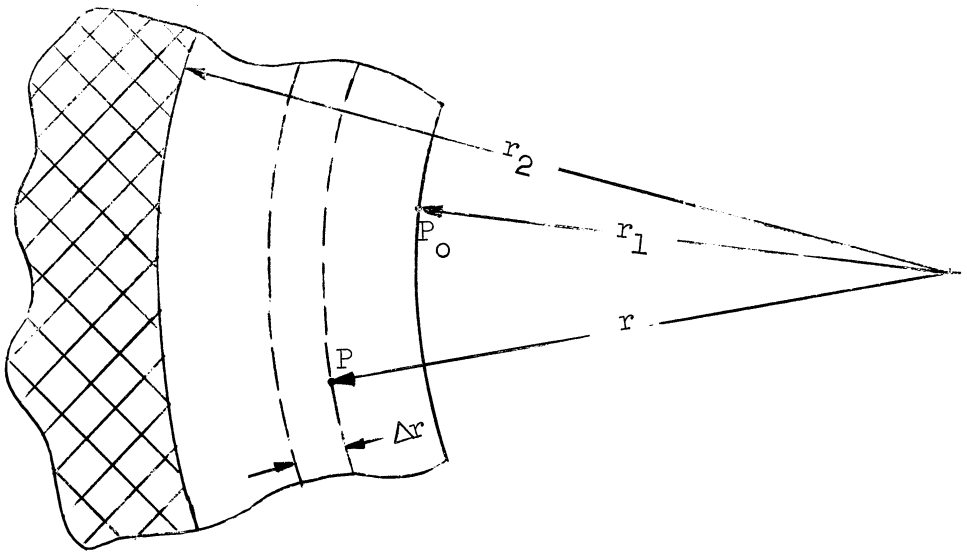

Let: r_2 = inside radius of evaporator, ft.

r_1 = radius at liquid-vapor interface, ft.

$r_2 - r_1 = x_o$, liquid film thickness, ft.

r = radius at a point in liquid film, ft.

ρ = density of liquid, lb_m/ft^3.

ω = angular velocity of evaporator, radians/sec.

F = centrifugal force acting on liquid at $\underline{r}$, lb_f.

P = centrifugal pressure acting on liquid at $\underline{r}$, lb_f/ft^2.

S = lateral area perpendicular to $\underline{F}$ at $\underline{r}$, ft^2.

h = height of liquid film in evaporator, ft.

dm = differential mass of liquid at $\underline{r}$ in annulus of thickness $\underline{dr}$, lb_m.

dV = differential volume of liquid at $\underline{r}$ in annulus of thickness $\underline{dr}$, ft^3.

g_c = conversion factor, 32.2 $lb_m ft/sec^2 lb_f$

$$dF = \frac{a\,dm}{g_c} = \frac{\omega^2 r\,dm}{g_c} = \frac{\omega^2 r \rho\, dV}{g_c} = \frac{\omega^2 r \rho \cdot 2\pi r h dr}{g_c};$$

$$dP = \frac{dF}{S} = \frac{\omega^2 r \rho \cdot 2\pi r h dr}{g_c \cdot 2\pi r h} = \frac{\omega^2 r \rho dr}{g_c}.$$

Integrating:

$$P - P_0 = \frac{\omega^2 \rho}{2 g_c}(r^2 - r_1^2)$$

$$= \frac{\omega^2 \rho (r - r_1)(r + r_1)}{2 g_c}.$$

For

$$r_2 - r_1 = x_0 \ll r_2,\ r_2 + r_1 \approx 2 r_2,$$

and:

$$P - P_0 \approx \frac{\omega^2 \rho x r_2}{g_c} = \frac{\rho x r_2}{g_c}(RPM)^2 \left(\frac{2\pi}{60}\right)^2, \quad \text{where } x = r - r_1.$$

APPENDIX C

COMPUTATION OF APPROXIMATE COUNTING EFFICIENCY
OF ION EXCHANGE SYSTEMS

1. Cylindrical Annular Geometry

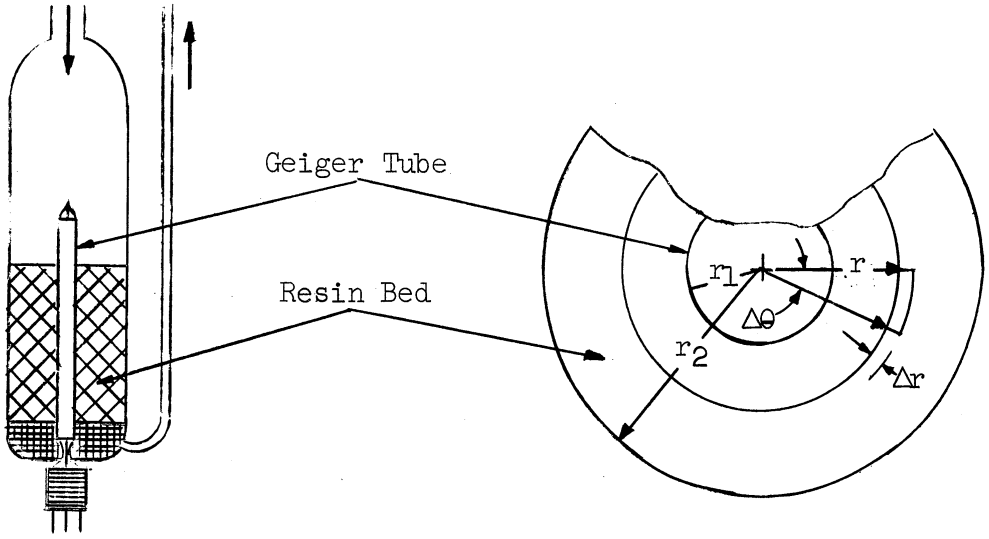

The computations are based upon the following assumptions:

1. All the strontium-89 is absorbed in a plane of infinitesimal thickness, and the distribution of activity in the plane is uniform.
2. The beta particles are emitted isotropically in the plane from an infinite number of point sources, and all beta particles emitted move entirely within the plane prior to their first scattering.
3. Beta particles are removed from the plane by scattering which follows an exponential decay law; neither a beta particle scattered from the plane nor bremsstrahlung is counted by the detector.

Let: C = total Sr++89 activity in resin bed, curies.

r_1 = outer radius of Geiger tube detector, cm.

r_2 = outer radius of resin bed, cm.

A = total absorption area = $\pi(r_2^2 - r_1^2)$, cm^2.

S = Sr++89 activity per unit area = $C/\pi(r_2^2 - r_1^2)$, curies/cm^2.

A = area of small sector of A = $r\Delta\theta\Delta r$, cm^2.

The activity in ΔA is:

$$Sr\Delta r\Delta\theta = \frac{C}{\pi(r_2^2 - r_1^2)} r\Delta r\Delta\theta$$

The fraction, α, of this activity that starts out in the direction of the Geiger tube is computed:

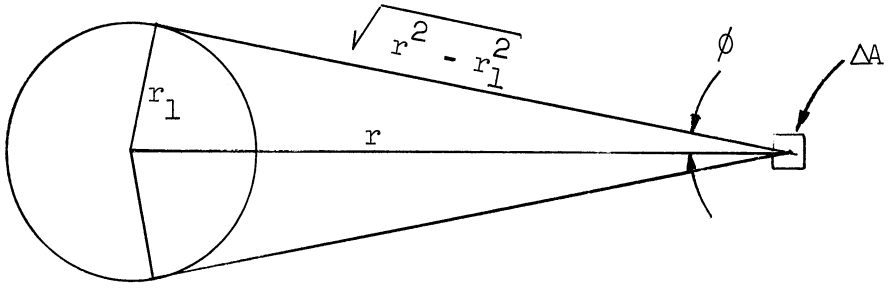

$$\alpha = \frac{2\phi}{2\pi} = \frac{\phi}{\pi} = \frac{1}{\pi} \text{ arc } \sin\left(\frac{r_1}{r}\right)$$

Thus, the total activity starting out from ΔA in the direction of the Geiger tube is:

$$\frac{C}{\pi(r_2^2 - r_1^2)} r\Delta r\Delta\theta \frac{1}{\pi} \arcsin\left(\frac{r_1}{r}\right) = \frac{C}{\pi^2(r_2^2 - r_1^2)} \arcsin\left(\frac{r_1}{r}\right) r\Delta r\Delta\theta.$$

But in going to the counting tube the fraction:

$$e^{-\mu\bar{r}}$$

of beta particles are scattered out of the beam. It is first necessary to evaluate $\bar{r}$. A rigorous analysis of this problem leads to a solution involving a nonelementary integral. As an approximation, the arithmetic

mean of the maximum and minimum distances from ΔA to the Geiger tube is employed:

$$\bar{r} \approx \frac{(r-r_1)+\sqrt{r^2-r_1^2}}{2} .$$

The total activity reaching the Geiger tube from ΔA is:

$$\frac{C}{\pi^2(r_2^2-r_1^2)} r \exp\left\{-\frac{\mu}{2}\left[(r-r_1)+\sqrt{r^2-r_1^2}\right]\right\}\arcsin\left(\frac{r_1}{r}\right)\Delta r \Delta\theta .$$

The total activity, J, reaching the counting tube is:

$$J = \frac{C}{\pi^2(r_2^2-r_1^2)}\int_{r_1}^{r_2} r \exp\left\{-\frac{\mu}{2}\left[(r-r_1)+\sqrt{r^2-r_1^2}\right]\right\}\arcsin\left(\frac{r_1}{r}\right)dr\int_0^{2\pi} d\theta .$$

$$= \frac{2C}{\pi(r_2^2-r_1^2)}\int_{r_1}^{r_2} r \exp\left\{-\frac{\mu}{2}\left[(r-r_1)+\sqrt{r^2-r_1^2}\right]\right\}\arcsin\left(\frac{r_1}{r}\right)dr .$$

The counting efficiency, η, is:

$$\eta = \frac{J}{C} = \frac{2}{\pi(r_2^2-r_1^2)}\int_{r_1}^{r_2} r \arcsin\left(\frac{r_1}{r}\right)\exp\left\{-\frac{\mu}{2}\left[(r-r_1)+\sqrt{r^2-r_1^2}\right]\right\}dr .$$

For the geometry of the counting system studied, the efficiency is computed as follows:

$$r_1 = 1.00 \text{ cm.}, \quad r_2 = 1.75 \text{ cm.}$$

The absorption coefficient for the beta particles emitted by strontium-89 is computed from experimental aluminum absorption data, and is found to be:

$$\frac{\mu}{\rho} = 7.65 \text{ cm}^2/\text{gm.}$$

For the resin-water mixture, $\rho = 1.00$ gm/cm^3. Then:

$$\mu = \left(\frac{\mu}{\rho}\right)\rho = 7.65 \times 1.00 = 7.65 \text{ cm}^{-1}$$

The integral is evaluated graphically:

r	arc $\sin(\frac{r_1}{r})$	$(r - r_1)$	$r^2 - r_1^2$	α*	$e^{-\alpha}$	I**
1.00	1.570	0	0	0	1	1.57
1.02	1.374	0.020	0.202	0.850	0.428	0.601
1.05	1.261	0.050	0.320	1.417	0.243	0.322
1.12	1.103	0.120	0.505	2.395	0.0913	0.113
1.25	0.926	0.250	0.752	3.840	0.0215	0.0249
1.45	0.763	0.450	1.050	5.75	0.0032	0.0035
1.75	0.609	0.750	1.437	8.41	negl.	negl.

* $\alpha = \frac{\mu}{2}\left[(r-r_1)+\sqrt{r^2-r_1^2}\right]$

** $I = r \arcsin\left(\frac{r_1}{r}\right) \exp\left\{-\frac{\mu}{2}\left[(r-r_1)+\sqrt{r^2-r_1^2}\right]\right\}$

$$\int_{1.00}^{1.75} r \arcsin\left(\frac{r_1}{r}\right) \exp\left\{-\frac{\mu}{2}\left[(r-r_1)+\sqrt{r^2-r_1^2}\right]\right\} dr = 0.0604.$$

$$\eta = \frac{2(0.0604)(100\%)}{\pi(1.75^2 - 1.00^2)} = 1.87\%.$$

2. Sandwich Geometry

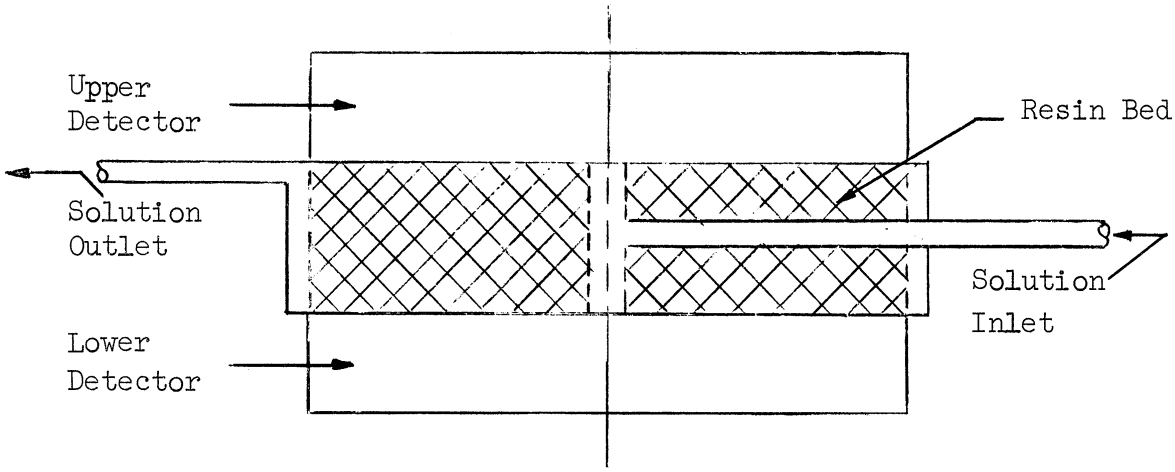

Assume:

1. An activity gradient that is a linear function of r, the distance from the z-axis. Then the activity per unit volume, a, is:

$$a = mr + b$$

where:

$$\text{at } r = 0,\ a = a_o \text{ and at } r = R,\ a = 0.$$

Therefore:

$$a_o = b, \text{ and } 0 = mR + a_o, \text{ or } m = -\frac{a_o}{R}.$$

Thus:

$$a = a_o - \frac{a_o}{R}r = \frac{a_o}{R}(R - r).$$

The value of a_o is determined from the following condition. Let C be the total activity of the resin bed. Then:

$$\int_V a\,dV = C$$

$$\int_V \frac{a_o}{R}(R-r)\,dV = \frac{a_o}{R}\left[R\int_V dV - \int_V r\,dV\right] = C\ ;$$

$$R\int_V dV = \pi R^3 h.$$

Using cylindrical coordinates:

$$\int_V r\,dV = \int_{-\frac{h}{2}}^{\frac{h}{2}} dz \int_0^{2\pi} d\theta \int_0^R r \cdot r\,dr = \frac{2\pi R^3 h}{3}.$$

Thus:

$$a_0 = \frac{3C}{\pi R^2 h},$$

and

$$a = \frac{3C}{\pi R^3 h}(R - r).$$

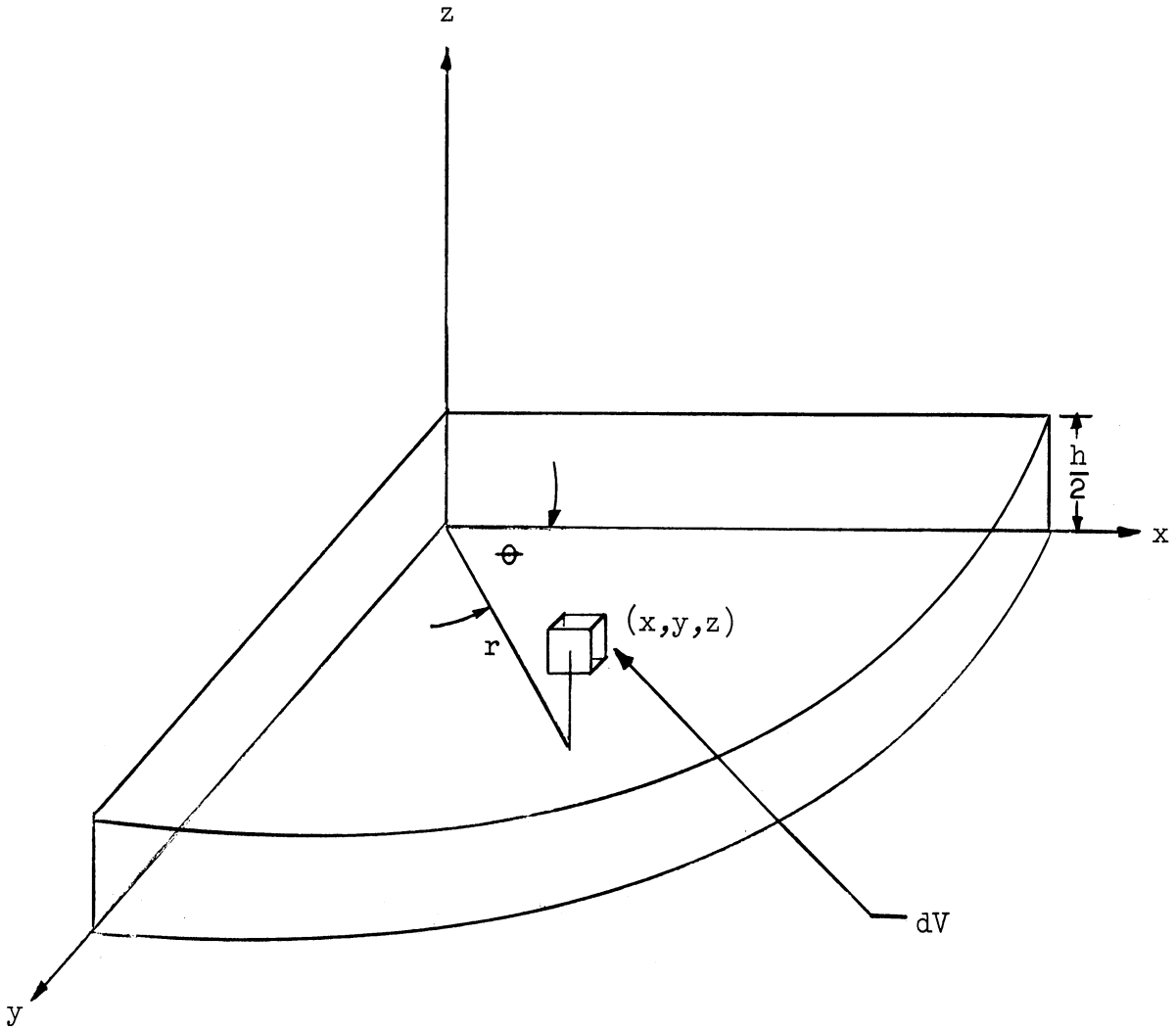

The number of particles emitted from dV per unit time is:

$$\frac{3C}{\pi R^3 h}(R - r)rdrd\theta dz.$$

If no scattering occurred, the probability of any beta particle reaching one of the two counters would be close to unity.

Assume:

2. The probability above is exactly unity.

The fraction of beta particles leaving dV that are ultimately detected is approximated. A plane parallel to the x-y plane is visualized as passing through the point (x,y,z) in dV. Half of the beta particles travel in the (+z) direction, and the other half travel in the (-z) direction. If $\bar{r}_1$ is the average distance a beta particle would go in travelling from dV to the upper counter, and $\bar{r}_2$ is the average distance a particle would go in travelling from dV to the lower counter, then the number of particles from dV that are counted per unit time is:

$$\frac{3C}{\pi R^3 h}(R-r)r\,dr\,d\theta\,dz \cdot \frac{1}{2}(e^{-\mu \bar{r}_1} + e^{-\mu \bar{r}_2})$$

$$= \frac{3C}{2\pi R^3 h}(R-r)r\left(e^{-\mu \bar{r}_1} + e^{-\mu \bar{r}_2}\right)dr\,d\theta\,dz.$$

The values of $\bar{r}_1$ and $\bar{r}_2$ are approximated as follows. The minimum value of r_1 is $(\frac{h}{2} - z)$.

Assume:

3. $\bar{r}_1 = k(\frac{h}{2} - z)$, $k > 1$ and $k = f(r,\theta,z)$.

4. $\bar{r}_2 = k(\frac{h}{2} + z)$.

The total activity, J, reaching the counters is:

$$J = \frac{2.3C}{2\pi R^3 h}\int_0^{h/2}\left[e^{-\mu k\left(\frac{h}{2}-z\right)} + e^{-\mu k\left(\frac{h}{2}+z\right)}\right]dz \int_0^{2\pi} d\theta \int_0^{R}(R-r)\,r\,dr$$

$$= \frac{2.6C}{R^3 h}\int_0^{h/2} e^{-\frac{\mu k h}{2}}\left[e^{\mu k z} + e^{-\mu k z}\right]\frac{dz}{2}\int_0^{R}(Rr - r^2)\,dr$$

$$= \frac{2C\,e^{-\frac{\mu k h}{2}}}{h}\int_0^{h/2}\cosh(\mu k z)\,dz = \frac{2C\,e^{-\frac{\mu k h}{2}}}{\mu k h}\int_0^{\frac{\mu k h}{2}}\cosh\phi\,d\phi$$

$$= \frac{C\,e^{-\frac{\mu k h}{2}}\sinh\left(\frac{\mu k h}{2}\right)}{\frac{\mu k h}{2}} = \frac{C(1-e^{-\lambda})}{\lambda}$$

where

$$\lambda = \mu k h$$

Thus:

$$\eta \equiv \frac{J}{C} = \frac{1-e^{-\lambda}}{\lambda}$$

As an example, assume the conditions of the cylindrical annular computation:

1. Strontium-89 cations absorbed on same ion exchange resin (ρ = 1.00 gm/cm^3)
2. $h = r_2 - r_1 = 1.750 - 1.000 = 0.750$ cm.
3. Assume here that k = 1.30.

Thus, $\lambda = \mu k h = 7.65 \times 1.30 \times 0.750 = 7.47$

$$\eta = \frac{1-e^{-7.47}}{7.47} \times 100\% = 13.4\%\ .$$

The following points should be observed:

1. η is R-independent only because of Assumption 1. Choosing another gradient function could introduce R-dependence into the equation for η.
2. Multiple scattering of beta particles is neglected, as is bremsstrahlung. A consideration of these factors would lead to an increase in the value of η.
3. The parameter $\underline{k}$ may be evaluated experimentally using the above equation for η.
4. With any "reasonable" choice of $\underline{k}$, the counting efficiency of the sandwich geometry is considerably greater than the corresponding efficiency of the cylindrical annular geometry.

APPENDIX D

EFFECT OF HOLDUP VOLUME IN CONDENSER UPON COMPOSITION OF FEED TO COUNTING SYSTEM

The existence of a finite holdup volume in the condenser section of the centrifugal evaporator indicates that the specific activity of the effluent solution may differ from the specific activity of the entering vapor at any instant. In this section, an equation is derived to determine how much condensate must pass before the specific activity of the effluent is a given fraction of the specific activity of the vapor, with the following assumptions:

1. The flow is steady-state; that is, there is no increase or decrease in the holdup volume, and the vapor feed rate is constant.
2. The specific activity of the vapor feed is constant.
3. The condensed vapor mixes completely with the holdup volume of liquid at each instant of flow.

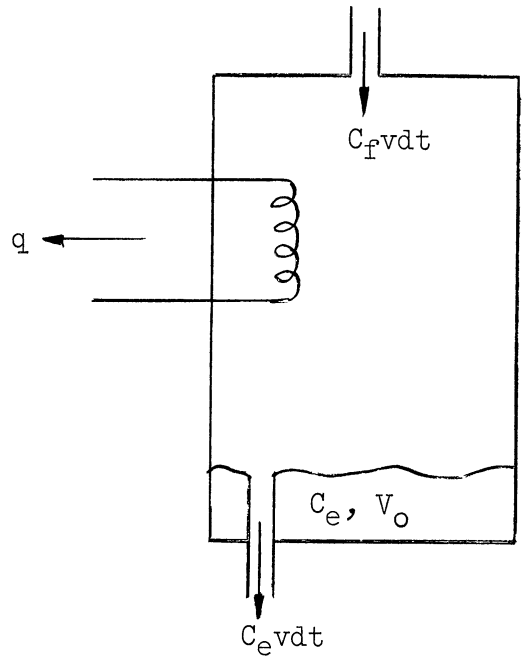

Let: V_o = holdup volume of condenser, ml.

C_o = initial specific activity of solution in condenser, curies/ml.

v = feed rate, ml/min.

C_f = specific activity of feed, curies/ml.

C_e = specific activity of effluent, curies/ml.

A differential activity balance at time t gives:

activity in - activity out = buildup in holdup volume

or:

$$C_f v\,dt - C_e v\,dt = d(C_e V_o) = V_o\,dC_e + C_e\,dV_o = V_o\,dC_e$$

$$(C_f - C_e)\,v\,dt = V_o\,dC_e$$

$$\int_0^t \frac{v}{V_o}\,dt = \int_{C_o}^{C_e} \frac{dC_e}{C_f - C_e}$$

$$\frac{v}{V_o}t = -\ln(C_f - C_e)\Big|_{C_o}^{C_e} = -\ln\left(\frac{C_f - C_e}{C_f - C_o}\right)$$

$$\frac{C_f - C_e}{C_f - C_o} = e^{-\frac{v}{V_o}t}.$$

Let: $C_o = 0$

and set $\alpha = C_e/C_f$

$$\frac{C_f - C_e}{C_f} = e^{-\frac{v}{V_o}t} = 1 - \alpha.$$

$$\alpha = 1 - e^{-\frac{v}{V_o}t}.$$

Here: V_o = 163.1 ml.

vt	α
0	0
50	0.263
100	0.458
200	0.707
300	0.841
400	0.914

V_o = 163.1 ml (Continued)

vt	α
500	0.954
600	0.975
700	0.986
800	0.993
900	0.996
1000	0.998
1500	1.000

APPENDIX E

REPRODUCTION OF DATA FROM NOTEBOOK FOR A TYPICAL RUN

March 7, Run Ia, 700 RPM, Four Heaters On

Coolant H_2O on. Four-liter flush begun. Electronics calibrated.
Co-60 count made: 25,579/3.00 = 8,526 cpm.
Background taken: 869/15.00 = 57.9 cpm.
250 ml of condenser H_2O passed through counting system.
Count rate = 863/15.00 = 57.6 cpm.
Coolant air on.

Time	T_{top}	T_{bot}	T_{ft}	Feed Rot	Mon Rot	RPM	I/V	Remarks
0944	73	73	70					Heaters 1-4 on.
0946								Evap. on.
0948	139	109						
0952	153	142						
0957	186	171						Pump on.
1010	183	204	140	0.14	0	631	1.70/72.5	
1020	199	221	170	0.14	0	687	1.62/72	
1030	214	234	185	0.14	flow	722	1.58/71	Opn. smooth.
1040	229	241	194	0.155	3.2	708	1.55/70	Begin bkgrnd.
1050	233	242	196	0.150	3.3	711	1.52/69	
1100	235	243	196	0.158	3.3	692	1.57/70	Incr. RPM.
1110	236	243	196	0.158	3.3	712	1.60/71	Begin Run
		bkgrnd = 1,536/28.00 = 54.8 cpm						
1120	236	243	196	0.158	3.3	707	1.57/71	Incr. RPM.
1130	237	243	197	0.156	3.3	677	1.72/75	
1140	237	243	197	0.153	3.4	695	1.71/75	Opn. smooth.
1150	237	243	197	0.153	3.4	712	1.71/75	
1200	237	243	197	0.152	3.4	696	1.68/74	
1210	237	243	197	0.153	3.4	702	1.68/74	End run; htrs. off.
		begin final count: 8,525/44.00 = 193.8 cpm						

Geiger counting of standard Feb. 19 soln. and feed soln.:
Voltage = 850 v; sample on second shelf from top

Std 1:	a.	64x75+56 = 4856	mean = 4870
	b.	64x76+20 = 4884	
Std 2:	a.	64x77+45 = 4973	mean = 4981
	b.	64x77+60 = 4988	
Ia1:	a.	64x90+41 = 5801	mean = 5837
	b.	64x91+49 = 5873	
Ia2:	a.	64x91+ 6 = 5830	mean = 5837
	b.	64x91+20 = 5844	

Mean Std. Count Rate = 4926x1.021
Mean Ia Count Rate = 5837x1.027

$$\text{Ratio} = \frac{5837 \times 1.027}{4926 \times 1.021} = 1.191$$

Calculation of Results of Run Ia:

A. Calculation of Specific Activity of Feed Solution (Ref. Feb. 19):

$$\frac{5.88 \text{ mc}}{5\text{x}10^{3} \text{ ml}} \text{ x } \frac{10^{-3}\text{c}}{\text{mc}} \text{ x } \frac{3.70\text{x}10^{10}\text{dis}}{\text{sec c}} \text{ x } \frac{60 \text{ sec}}{\text{min}} = 2.61\text{x}10^{6} \text{ cpm/ml}$$

The ratio of the feed solution to standard solution specific activity is 1.191. The feed solution specific activity is thus:

$2.61\text{x}10^{6}\text{x}1.191 = 3.11\text{x}10^{6}$ cpm/ml

Calculation of True Specific Activity of Condensate:

Final count rate = 193.8 cpm
Initial count rate = 54.8 cpm
Net count rate = 139.0 cpm

Time for run = 50.0 min.
Feed rate to counting system = 11.3 ml/min.

Measured Solution Specific Activity =

$$\frac{139.0}{(50.0)(11.3)} = 0.246 \text{ cpm/ml}$$

Corrected back to Feb. 19:

$0.246/0.816 = 0.301$ cpm/ml

Absolute Solution Specific Activity =

$0.301\text{x}43.5 = 13.09$ cpm/ml

The Decontamination Factor is =

$$\frac{26.1\text{x}10^{5}}{13.09} = 2.0\text{x}10^{5}$$

The mean RPM = 700.

BIBLIOGRAPHY

1. Lowe, C. S. et al. Decontamination of Liquid Wastes by Iron Sulfide, Iron Hydroxide, and Calcium Phosphate Precipitations. AECD-3632, Dec. 28, 1953.

2. Bates, R. L. and McEwen, M. Engineering Study of Evaporation for Concentrating Radioactive Liquid Wastes. AECD-4150, Nov. 1, 1950.

3. Cowan, F. P. and Nehemias, J. V. Sensitivity of Liquid Monitoring by the Evaporation Method. AECU-985, March 30, 1951.

4. Hall, K. L. Determination of (d,alpha) Reaction Cross Sections. AECU-3126, Sept. 21, 1955.

5. Manowitz, B. and Bretton, R. H. Progress Report on Waste Concentration Studies. III. Decontamination Efficiency of the Filtration Process. BNL-90, Oct. 1, 1950.

6. Horrigan, R. V. and Fried, H. M. Progress Report on Waste Concentration Studies. V. Engineering Results on the BNL Semi-Works Vapor Filtration Vapor Compression Evaporator. BNL-121, Aug. 15, 1951.

7. Quarterly Progress Report: July 1 - Sept. 30, 1954. BNL-314, 29.

8. Bretton, R. H. and Horrigan R. V. The Occurence and Control of Radioactive Entrainment in Evaporator Systems. BNL-1639, Oct. 1953.

9. Heath, R. L. Fission Product Monitoring in Reactor Coolant Streams. IDO-16213, Jan. 1, 1956, 75.

10. Project Summary Development of Laboratory Waste Disposal Unit. KLX-1389, May 1, 1953.

11. Nicholson, E. L. et al. Design and Initial Operation of the Radio-Chemical Waste Evaporator. ORNL-393, Sept. 22, 1949.

12. Borkowski, C. J. and Handley, T. H. Instrument Research and Development Quarterly Progress Report (for) Period Ending April 20, 1951. ORNL-1056, April, 1951.

13. Shank, E. M. ORNL Radiochemical Waste Evaporator Performance Evaluation, December 1949 Through December 1950. ORNL-1513, June 26, 1953.

14. Maximum Permissible Amounts of Radioisotopes in the Human Body and Maximum Permissible Concentrations in Air and Water. Handbook 52, U. S. Dept. of Commerce, National Bureau of Standards, March 20, 1953.

15. Isotope Catalog and Price List. Oak Ridge National Laboratory.

16. Rohm and Haas Co. Technical Bulletin IE-10-55(IR-120).

17. Rohm and Haas Co. Technical Bulletin IE-14-55(IRA-400).

18. Nachod, F. C. and Schubert, J. Ion Exchange Technology. New York: Academic Press, Inc., 1956, 24-25.

19. Lauderdale, R. A. and Emmons, A. H. "A Method for Decontaminating Small Volumes of Radioactive Water." J. Am. Water Works Assn., 43, 5, (May, 1951), 327.

20. Emmons, A. H. and Lauderdale, R. A. "Low Levels of Radioactive Contaminants in Water." Nucleonics, 10, 6, (June, 1952), 22.

21. Aiba, S. The Decontamination of Radioactive Liquid Wastes with a Centrifugal Evaporator. Michigan Memorial Phoenix Laboratory, University of Michigan, Ann Arbor, Michigan. May, 1957.

22. Ray, J. W. The Centrifugal Evaporator. Master's Thesis, University of Michigan, Ann Arbor, Michigan, 1957.

23. Schreiber, R. E. Theory of the Centrifugal Evaporator and its Application to the Processing of Fission Product Wastes. M. S. Thesis Requirement, University of Michigan, Nuc. Eng. Dept., Ann Arbor, Michigan, 1957.